



# Preparation and Mechanical Characterisation of Self-Compressed Collagen Gels

Master Thesis

by Charitini Andriakopoulou

**Parent Institution:** Delft University of Technology, Faculty of Mechanical, Maritime and Material Engineering

**Host Institution:** University of Strathclyde, Department of Biomedical Engineering

**Master Program:** Biomedical Engineering

**Specialization:** Tissue Biomechanics and Implants

**Student No:** 4315103

**Supervisor at Delft University of Technology:** Amir A. Zadpoor

**Supervisor at University of Strathclyde:** Philip E. Riches

**Period:** February 2015 – February 2016



This work was performed within the framework of my master thesis and internship project and will lead to the reward of a Master Degree in Biomedical Engineering of Delft University of Technology. The experimentation was performed at the Biomedical Department of University of Strathclyde and the work is subjected to evaluation at Delft University of Technology. All the experimental equipment that has been used for collagen concentration and mechanical characterization was constructed in the mechanical workshop of Biomedical Engineering Department, University of Strathclyde. The project was supervised by Amir Zadpoor, associate professor at Delft University of Technology, and Phil Riches, lecturer at University of Strathclyde.



## **Acknowledgements**

This work could not be completed if it was not for my supervisor Dr. Phil Riches who guided and advised me through all the stages of my research. His ideas inspired and motivated me and his lectures gave me insight into the mechanics of biphasic materials. I would also like to thank my other supervisor, Dr. Amir Zadpoor, for his feedback and his academic interest in my work. I could not forget Katie Henderson, laboratory assistant at University of Strathclyde, who showed me my way through the lab and taught me how to set collagen gels, and of course Stephen Murray, member of staff of the mechanical workshop (Biomedical Engineering Department, University of Strathclyde) who turned my drawings into real experimental equipment. Last but not least, I thank Davide Erbogasto, PhD candidate, for his precious help with electron microscopy and Peter Agbekoh, PhD candidate, who was always willing to answer my questions concerning biological aspects.



# Contents

ABSTRACT.....	11
1. Introduction.....	13
2. Materials and Methods.....	17
2.1 Gel Preparation.....	17
2.2 Concentration.....	17
2.3 Sampling.....	18
2.4 Estimation of Thickness.....	18
2.5 Surface Electron Microscopy (SEM).....	19
2.6 Unconfined Ramp Hold Compression.....	19
2.7 Estimation of Collagen Proportion.....	19
2.8 Finite Element Modelling (FEM).....	19
2.9 Parameter Optimisation.....	22
2.10 Statistical Analysis.....	23
2.11 Dynamic Loading.....	23
3. Results.....	25
3.1 Direct Measures of Gel Characteristics.....	25
3.2 Surface Electron Microscopy (SEM).....	27
3.3 Indirect Determination of Gel Characteristics.....	27
3.3.1 Model Prediction of Stress Relaxation.....	27
3.3.2 Material Parameters.....	29
3.3.3 Frequency Dependence of Phase Lag and Dynamic Modulus.....	29
4. Discussion.....	33
4.1 Collagen Gel Concentration.....	33
4.2 Unconfined Ramp Hold Compression.....	33
4.3 Dynamic Mechanical Analysis (DMA).....	37
4.4 Conclusion.....	38
4.5 Future Challenges.....	38
APPENDIX A.....	41
APPENDIX B.....	43
APPENDIX C.....	44
APPENDIX D.....	46
APPENDIX E.....	47

APPENDIX F.....	49
APPENDIX G.....	50
APPENDIX H.....	51
APPENDIX I.....	52
APPENDIX J.....	55
APPENDIX K.....	56
APPENDIX L.....	57
APPENDIX M.....	58
APPENDIX N.....	60
APPENDIX O.....	63
APPENDIX P.....	67
APPENDIX Q.....	71
APPENDIX R.....	73
APPENDIX S.....	77
REFERENCES.....	81

## TABLE OF FIGURES

Figure 1.1.1: Light micrograph showing the birefringence of a collagen sheet after unconfined PC ( <i>Brown, et al. 2005</i> ).....	15
Figure 2.2.1: Experimental setup for collagen gel concentration.....	20
Figure 2.4.1: Apparatus for measuring the thickness of plastically compressed gels.....	20
Figure 2.4.2: Indentation with and without sample.....	22
Figure 3.1.1: Collagen gel that has undergone confined self-compression for 18 hours.....	25
Figure 3.1.2: Percentage collagen proportion of plastically compressed collagen gels that originate from highly-hydrated gels of different concentration.....	26
Figure 3.1.3: Thickness and percentage induced strain of plastically compressed collagen gels of different concentration.....	26
Figure 3.1.4: Peak stress for plastically compressed collagen gels of different concentration undergone ramp hold compression.....	27
Figure 3.2.1: Scanning electron microscopy of the fluid leaving surface of a self-compressed gel of 3.2% collagen.....	28
Figure 3.2.2: Scanning electron microscopy of the top surface of a self-compressed gel of 3.2% collagen.....	28
Figure 3.3.1: Curve fitting of the force response to ramp hold unconfined compression of a 2.9% collagen sample.....	29

Figure 3.3.2: Young's modulus of plastically compressed collagen gels of different concentration.....	30
Figure 3.3.3: Zero-strain hydraulic permeability of plastically compressed collagen gels of different concentration.....	30
Figure 3.3.4: Phase lag ( $\delta$ ) dependence with frequency strain input for 3.2% (w/w) self-compressed collagen gels.....	31
Figure 3.3.5: Complex, storage and loss moduli dependence with frequency strain input for 3.2% (w/w) self-compressed collagen gels.....	31
Figure 4.2.1: Confined compression ramp hold test results. <i>Knapp, Barocas, Moon (1997)</i> .....	36
Figure 4.2.2: Confined ramp hold compression of a highly hydrated collagen gel. Unpublished source.....	37
Figure 4.5.1: A future evolvemnet: Experimental set-up for concentration of collagen gels using confined compression.....	39
Figure 5.5.1: Apparatus used for collagen solution casting.....	47
Figure 5.5.2: Acrylic porous plate.....	47
Figure 5.5.3: Collagen gel concentration method.....	48
Figure 5.6.1: Diagram showing the procedure that was followed to characterize plastically compressed collagen gels.....	49
Figure 5.7.1: Experimental setup for unconfined compression of collagen gels.....	50
Figure 5.8.1: FE model of a plastically compressed collagen gel under unconfined ramp hold compression.....	51
Box Chart 5.13.1: Peak surface stress for 2.9, 3.2 and 3.6% collagen samples.....	59
Figure 5.14.1: Scanning electron microscopy of the fluid leaving surface of a self-compressed gel of 3.2% collagen (5,000 times magnification).....	60
Figure 5.14.2: Scanning electron microscopy of the fluid leaving surface of a self-compressed gel of 3.2% collagen (10,000 times magnification).....	60
Figure 5.14.3: Scanning electron microscopy of the top surface of a self-compressed gel of 3.2% collagen (5,000 times magnification).....	61
Figure 5.14.4: Scanning electron microscopy of the top surface of a self-compressed gel of 3.2% collagen (10,000 times magnification).....	61
Figure 5.14.5: Scanning electron microscopy of the fluid leaving surface of a self-compressed gel of 2.9% collagen (5,000 times magnification).....	62
Figure 5.14.6: Scanning electron microscopy of the fluid leaving surface of a self-compressed gel of 3.6% collagen (5,000 times magnification).....	62
Figure 5.15.1: Image processing of the fluid leaving surface of a 3.2% collagen sample.....	63
Figure 5.15.2: Image processing of the top surface of a 3.2% collagen sample.....	64
Figure 5.15.3: Image processing of the surface fibrils of a 2.9% collagen sample.....	65
Figure 5.15.4: Fit of a histogram showing the frequency of different values for fibril radius.....	65
Figure 5.15.5: Parameters of the Extreme function. Source OriginLab.....	66
Figure 5.16.1: Curve fitting of the force response to ramp hold unconfined compression of a 2.9% collagen sample ( $R^2=0.976$ ).....	67

Figure 5.16.2: Curve fitting of the force response to ramp-hold unconfined compression of a 2.9% collagen sample ( $R^2=0.869$ ).....	67
Figure 5.16.3: Curve fitting of the force response to ramp-hold unconfined compression of a 3.2% collagen sample ( $R^2=0.981$ ).....	68
Figure 5.16.4: Curve fitting of the force response to ramp-hold unconfined compression of a 3.2% collagen sample ( $R^2=0.938$ ).....	68
Figure 5.16.5: Curve fitting of the force response to ramp-hold unconfined compression of a 3.6% collagen sample ( $R^2=0.954$ ).....	69
Figure 5.16.6: Curve fitting of the force response to ramp-hold unconfined compression of a 3.6% collagen sample ( $R^2=0.929$ ).....	69
Figure 5.16.7: Coefficient of determination ( $R^2$ ) for the fits of stress relaxation of collagen gels of different concentration.....	70
Figure 5.17.1: Fluid pressure (first column) and fluid flux (second column) gradients in a 3.2% collagen gel undergoing unconfined ramp-hold compression.....	71-2
Box Chart 5.18.1: Young's modulus, zero-strain hydraulic permeability and non-linear permeability coefficient for 2.9, 3.2 and 3.6% collagen samples.....	76
Figure 5.19.1: Dynamic loading of a 3.2% collagen gel at 0.1Hz frequency.....	77
Figure 5.19.2: Fit of experimental data obtained from dynamic loading of a 3.2% collagen gel at 0.1Hz frequency.....	77
Figure 5.19.3: Dynamic loading of a 3.2% collagen gel at 5Hz frequency.....	78
Figure 5.19.4: Fit of experimental data obtained from dynamic loading of a 3.2% collagen gel at 5Hz frequency.....	78

## TABLE OF TABLES

Table 5.8.1: Time stepping parameters of the FE analysis.....	51
Table 5.11.1: Percentage collagen proportion of samples that originate from 0.2, 0.3 and 0.4% collagen gels.....	56
Table 5.12.1: Thickness measurements of concentrated collagen samples.....	57
Table 5.13.1: Peak surface stress of 2.9, 3.2 and 3.6% collagen samples.....	58
Table 5.18.1: Material's parameters and determination coefficient ( $R^2$ ) for 2.9% collagen samples.....	73
Table 5.18.2: Material's parameters and determination coefficient ( $R^2$ ) for 3.2% collagen samples.....	74
Table 5.18.3: Material's parameters and determination coefficient ( $R^2$ ) for 3.6% collagen samples.....	75
Table 5.19.1: Phase lag ( $\delta$ ), complex, storage and loss moduli of a 3.2% collagen gel at different frequencies.....	79

## ABSTRACT

Collagen gels hold great promise in the field of tissue engineering as collagen is highly biocompatible, biodegradable, abundant in nature and it provides an optimum environment for tissue regeneration and restoration of normal tissue function. However, collagen hydrogels have poor mechanical strength due to low collagen proportion and thus are not capable of substituting native tissue without special treatment. The latter usually involves methods that impart some degree of cytotoxicity and impede optimal regeneration.

In this study, hyper-hydrated collagen gels were concentrated without using any method that reduces cellular activity. Gels were left to self-compress in a laterally confined manner for a considerable period of time to expel excessive interstitial fluid and to transform to relatively concentrated collagen sheets. These collagen constructs may be seeded with cells and constitute an excellent starting material for building a tissue.

The main goal of the study is to create and mechanically characterise self-compressed collagen gels, identifying the mechanical effect of expelling fluid by taking into account their two-phase nature. Plastically compressed collagen gels of three different concentrations were tested under unconfined ramp hold compression assuming biphasic theory. A finite element (FE) model was developed to simulate the experiment and analyse results by numerically fitting a solution to experimental data. The FE model was fitted to the experimental results using a numerical iteration algorithm to predict the values of material parameters. The collagen matrix was modelled as a neo-Hookean material, isotropic and homogeneous. Permeability of collagen gels was assumed to follow the strain dependency of Lai and Mow (1980). Collagen samples were also tested under dynamic loading to explore the frequency dependence of phase lag ( $\delta$ ), storage and loss modulus.

Results indicate that after confined self-compression for 18 hours, collagen density of gels increased almost 10 times, Young's modulus ranged from 0.76-1.1kPa and zero-strain hydraulic permeability decreased from 51 to 21 mm<sup>4</sup>/Ns with increasing collagen content. The FE model coupled with the optimisation algorithm can detect differences in material parameters among gels of different collagen concentration and can reveal the poromechanics during loading. Further, dynamic mechanical analysis (DMA) revealed a profound increase of phase lag ( $\delta$ ) and dynamic modulus with increasing frequency.

The present work is the first work that studies the mechanical properties of concentrated collagen gels using biphasic theory. It constitutes a strong base from which more complex constitutive behaviour can be applied to the FE model. Although, the collagen concentration method via confined self-compression that was adopted did not result in collagen constructs strong enough to substitute native tissue, further compression of those materials in a laterally confined controllable manner could increase collagen density and mechanical properties, even in the range of body tissues.



# Introduction

Tissue engineering manipulates the native mechanisms of our body to achieve optimal tissue repair and restoration of normal cellular and overall activity. (Tabata 2009) Collagen, a natural polymer known for its outstanding biocompatibility and ability to promote cellular growth, was originally proposed as substrate for cell culture in 1956 by Ehrman and Gey. Today, collagen, alone or in combination with another material, may be used as scaffold for cell attachment in skin (Blais, et al. 2013), bone (Cui, Li and Ge 2007), cartilage (Chiang and Jiang 2009), ligament and tendon (Kew, et al. 2011), vascular (Thottappillil and Nair 2015), nerve (Siemionow, Bozkurt and Zor 2010), corneal (Willoughby, Batterbury and Kaye 2002) and dural (Zerris, et al. 2007) tissue engineering.

Purified collagen usually of animal origin (mammalian or marine) may be processed in such a way to create a collagenous scaffold that can be seeded with cells and get implanted into the human body. However, the physicochemical methods used to purify collagen ultimately alter the native structure by disassembling its fibrillar network. Purified collagen can be put to self-assembly (i.e. to form fibrils) and develop its biphasic nature, a procedure called fibrillogenesis. During fibrillogenesis, fibrils develop weak non-covalent bonds that are responsible for holding the collagen structure together. However, collagen lattice is still weak and readily deformable compared to naturally formed collagen. (Brown, et al. 2005), (Kew, et al. 2011), (Lai, Anderson and Fuller 2011), (Ratner, et al. 1996), (Rich, et al. 2014)

Collagen hydrogels are biphasic materials that consist of a mixture of a porous permeable solid, an insoluble network of fibrils (the collagen matrix) and the interstitial fluid. Prepared from collagen solutions of typically 2-5 mg/ml, they contain extremely low collagen proportion (0.2-0.5% collagen in more than 99.5% fluid). This excess water content is predominantly responsible for their poor mechanical properties. Accordingly, collagen hydrogels are unstable and not sufficiently strong to be used as scaffolds in tissue engineering. (Brown, et al. 2005), (Cheema and Brown 2013), (Saddiq, Barbenel and Grant 2009) Several approaches have been devised to enhance them, including chemical (Zeeman 1998), physical (Rich, et al. 2014) and enzymatic (Orban, et al. 2004) crosslinking, addition of cells (Saddiq, Barbenel and Grant 2009) and glycosaminoglycans (GAGs) (Matsuda, et al. 1990), reinforcement with fibers of natural (Gentleman, et al. 2003) or synthetic (Jeong, et al. 2007) origin. However, these approaches either impart toxic effects on cells or do not result in sufficiently strong gels. (Orban, et al. 2004) (Saddiq, Barbenel and Grant 2009)

Collagen hydrogels tend to lose fluid under the force of gravity when in unconfined or laterally confined state. They can expel half of their initial weight in only 2 hours of self-compression. More rapid fluid loss can be achieved by using blotting paper or PC. (Neel, et al. 2006) Fluid loss leads to reallocation of the solid and fluid volume fractions. Gels become more concentrated, stiffer and they present a more elastic behaviour. The simplest way to concentrate collagen hydrogels is by self-compression.

In 2005, Brown, et al. compressed collagen gels in unconfined creep in order to increase the collagen fibril density (CFD) and consequently to create a stiffer material that would closely mimic native collagen. Authors applied a uniform pressure of 1.1kPa for 5 minutes and they transformed from highly-hydrated gels of 3.6mm initial thickness to collagen sheets of 35 $\mu$ m

average thickness (99% strain) and 18% collagen. Final construct composition can be compared to some pre-maturity connective tissues. (Brown, et al. 2005) Unconfined plastic compaction (PC) can increase CFD by more than 40 times by expelling up to 95 wt% of the interstitial water and produce anisotropic structures. (Neel, et al. 2006) The major advantages of this method are the simplicity, the non-cytotoxicity and the short time needed (within minutes) to concentrate gels. Researchers have explored the potential of plastically compressed gels in clinical application. In 2012, Ghezzi et al. fabricated collagenous hollow tubes utilizing the PC protocol developed by Brown, et al. (2005); mechanical characterization indicated great potential to be used as vascular grafts. Chicatun, et al. (2011) created collagen/chitosan hybrid plastically compressed gels intended to be used as osteoid-mimicking scaffolds in bone tissue engineering. Marelli, et al. (2011) concluded that increase in CFD through PC increases the mineralization potential of collagen gels.

Nevertheless, current unconfined PC methods lack control as fluid expulsion cannot be limited in only one direction and final constructs are not homogeneously compacted. Collagen fibrils located closer to the water outlet found to be more concentrated than fibrils located far from the fluid-leaving surface (Figure 1.1.1) and that CFD was different between the body and the edges of the construct (Brown, et al. 2005) indicating that fluid loss occurred not only through the lower surface of the gel but also through the lateral edge. Confined PC, on the other hand, is a highly controllable experiment that can limit fluid expulsion to just one surface. Since equilibrium has been reached, biphasic theory predicts zero axial strain gradient, i.e. homogeneously compacted collagen sheets.

The collagen matrix forms interconnected pores and fluid is free to move through the pores influencing the mechanical response upon loading. Each constituent (fluid and solid) is incompressible, but their mixture may change in volume as fluid is free to move through the interconnected pores of the collagen network. The only theory that accounts for the interaction between the solid and the fluid phase is biphasic theory. Biphasic theory is based on basic principles and laws of physics to study the mechanical behaviour of two-phase tissues.

Unlike tension and shear, in compression, the behaviour of collagen gels is dependent on the fluid movement relative to the solid matrix. The fluid flow creates a drag force that is acting on the solid matrix. The solid matrix resists by generating a stress field that is dependent both on the magnitude of the interstitial drag and on the intrinsic properties of the solid matrix. Compression is a suitable experiment to study biphasic materials as the interaction between the hyper-elastic behaviour of the solid matrix and the viscous properties of fluid phase become relevant.

A property that must be taken into account when designing a tissue-engineered material is permeability. Permeability refers to the ability of a porous material to transmit fluids. It is related to mechanical properties and microstructure, as well as the ability of mass transfer (i.e. convection and diffusion of oxygen, nutrients, waste and other molecules) and cell migration. (Serpooshan, et al. 2010), (Serpooshan, et al. 2013). It is believed that cells themselves decrease permeability by occluding the pores. Permeability is usually measured by studying the fluid flow through a porous material under a known hydrostatic pressure. However, gels are quite fragile materials and can easily get damaged. To deal with experimental limitations, a number of models have been developed to predict the permeability of porous materials. (Happel 1959) (Ramanujan, et al. 2002) (Swartz and Fleury 2007) Experimental data can get curve-fitted with numerical solutions obtained from theoretical or empirical models and permeability may be deduced. (Busby, et al. 2013) (Gu, et al. 2003) (Serpooshan, et al. 2013)

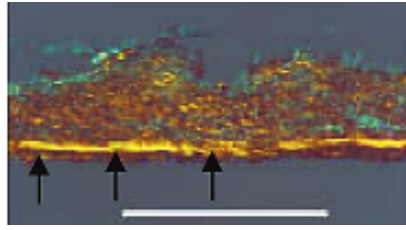


Figure 1.1.1: Light micrograph showing the birefringence of a collagen sheet after unconfined PC. A dense lamella layer is located parallel to the fluid-leaving surface while minor layers are located throughout the body of construct. Scale bar: 50 $\mu$ m (Brown, *et al.* 2005)

Collagen gels may also be characterized in dynamic loading. Tissues like bone and cartilage are exposed to such loads on daily basis, e.g. walking, running etc. The response of such materials depends on the frequency of the input (that can be stress or strain). Experimentally, we may vary the frequency and measure the tissue displacement or the surface stress. It has been proposed that for small strains (<15%) collagen gels behave more like a Maxwell fluid. (Chandran and Barocas 2004)

The aim of this study is to develop and characterise concentrated collagen gels using biphasic theory. The protocol of confined self-compression that was followed to concentrate collagen hydrogels is a controllable method that provides homogeneously compacted gels. Secondary aim is to explore the viscoelastic properties of self-compressed collagen gels by testing in dynamic loading.



# Materials and Methods

## 2.1 Gel Preparation

Type I collagen (5.92 mg/ml) was prepared from rat tail tendon. The tendons were immersed into 0.5M acetic acid and left for 48h at 4°C. The collagen was filtered, dialysed against 0.1X DMEM for 24h at 4°C and sterilized by centrifugation (10,000 rpm for 2h at 6°C). Collagen concentration (Y) was measured by desiccation for 5 days at 37°C. Fifty millilitres of collagen solution were prepared by following the below-cited protocol:

- $\frac{10(N \times X)}{Y}$  ml collagen
- $\frac{N}{10}$  ml DMEM (10X DMEM:NaOH, 2:1 mixture)
- $N - \frac{10(N \times X)}{Y} - \frac{N}{10}$  ml 1/1000 (v/v) acetic acid

where  $N$  is the number of millilitres of the collagen solution and  $X$  is the collagen proportion of the collagen solution (0.2 for a 0.2% gel, 0.3 for a 0.3% gel etc). Fibrillogenesis and gel formation were triggered by pH adjust to 8-8.5 by dropwise addition of 1M NaOH. After preparation, the gel mix was quickly casted into a custom-made mould (see paragraph 2.2) and left to self-compress for 2 hours at room temperature.

## 2.2 Concentration

Highly hydrated collagen gels were concentrated by self-compression in a confined manner. The apparatus that was used for confined self-compression is described in this paragraph.

Gel solution was casted in a custom-made apparatus that consists of an acrylic tube (70mm internal diameter, millilitre scaled) with a rubber O-ring to prevent leakage (part A) and an acrylic plate (part B). Part A and B are connected with bolts and serve as a mould. For impeding the gel to be in direct contact with the acrylic plate, a plastic membrane was applied before casting.

After gelation, a plug (made of acetal), which is able to slide in and out of part A, was inserted until it was in contact with the gel (touching but not compressing). All the equipment was turned upside down. Plug stayed in place due to frictional forces and acted as gel's support. Part B and plastic membrane were removed. The gel was detached from the walls using a scalpel. First, a nylon mesh layer (100 micron aperture) was placed on top of the collagen gel, then a filter paper, a porous plate (Figure 5.5.2), and finally an acrylic tube (part C). All the equipment was turned upside-down once more and the plug was removed. The nylon mesh

prevents paper and gel to be in direct contact. The filter paper allows fluid to leave the tissue but not collagen fibrils. Fluid expulsion occurred through the bottom surface (fluid leaving surface). (Figure 2.2.1)

Fifty millilitres of highly-hydrated collagen gel were left to self-compress for 18 hours at 20°C. By using this concentration method, highly hydrated and structurally unstable gels transformed to thin collagen sheets that are able to sustain their own weight. After self-compression, the samples were immersed in PBS to become maintain hydration. The procedure of concentration via confined self-compression was repeated for each 0.2, 0.3 and 0.4% (w/v) collagen gels.

## 2.3 Sampling

A hole punch of 8mm in diameter was used to extract collagen samples. Thirteen samples were obtained per each self-compressed collagen sheet of initially 0.2, 0.3 and 0.4% collagen. One sample was used for estimation of thickness immediately after self-compression. Subsequently, ten samples were tested in stress-relaxation assuming the thickness measured from the first sample. Those ten samples were also used for estimation of collagen proportion (solid volume fraction). Force-time data obtained from stress-relaxation and solid volume fraction were used to estimate material parameters. Last two samples were fixed for imaging. Samples were immersed in 4% formaldehyde for 20 minutes to suppress any biological activity and were stored for future imaging.

Subsequently, 50 millilitres of gel of 0.3% collagen were produced following the same procedure and six specimens of 8 mm diameter were extracted using the hole punch. One specimen was used for measuring samples' thickness and the rest were tested in dynamic loading.

The thickness of all the 70mm-in-diameter collagen sheets was greater close to the circumferential boundary due to the design of the porous plate (i.e. less holes at the circumferential boundary). Thus, samples were not taken close to the boundary.

## 2.4 Estimation of Thickness

The thickness of the plastically compressed gels was measured by perforating a collagen sample (that had been extracted from the centre of the 70mm-collagen sheet) with a custom-made indenter (Figure 2.4.1) that was displacement controlled by a BOSE Electroforce® 3200 Test Instrument (BOSE, UK) accompanying by WinTest® software. A 250g load cell and a 1Hz load filter were used to measure force response. When the indenter perforated the sample, a small force reading  $F_i$  is acquired on entering the sample's surface and a relatively large force reading  $F_j$  is acquired on touching the sample's support. The displacement of the indenter between those two force measurements corresponds to the sample's thickness. Five measurements were taken from different areas of the same sample and the average was assumed as the sheet's thickness.

In Figure 2.4.2, the difference in force reading with (A) and without (B) sample becomes relevant. A rate of as high as 0.1mm/sec was chosen for the indentation as a slower rate would involve viscoelastic effects. The entering and exiting point measurements were deduced by comparing indentation data obtained with and without sample for each thickness measurement.

## 2.5 Surface Electron Microscopy (SEM)

Two sample per each group 0.2%, 0.3% and 0.4% collagen gel were examined using scanning electron microscopy (SEM). Samples were prepared by gradually dry them in ethanol (70%, 90%, 95% and 100%) for 1 minute and then treat them using gold sputtering to become electrically conductive using a vacuum sputter (Bio Rad, SEM Coating System). The collagen meshwork of both the upper and the lower fluid leaving surface was observed under 5,000 and 10,000 times magnification using a scanning electron microscope (TM-1000 Hitachi). The images were processed using ImageJ to estimate pore size and fibril diameter.

## 2.6 Unconfined Ramp Hold Compression

A ramp hold unconfined compression was considered a suitable technique to study the mechanical behaviour of those thin plastically compressed collagen gels. Samples were placed on an impermeable flat support which was attached to a 250g load cell and were compressed by a rigid cylinder. Both the lower support and the impermeable surface of the rigid cylinder were coated with wet and dry paper (1200 grit) to prevent gel slippage. The rigid cylinder was displacement controlled by a BOSE Electroforce<sup>®</sup> 3200 Test Instrument (BOSE, UK) accompanying by WinTest<sup>®</sup> software. A force filter of 10Hz was used to neglect large ambience frequencies.

Ten collagen samples per each group were tested in ramp-hold compression. Samples' surface was found by lowering the rigid cylinder until a force reading of 0.25g (stress equivalent to 48.8Pa) was achieved. Samples were left for 2 minutes to equilibrate. Pre-stressed specimens were then compressed by 10% at a ramp rate of 1%/sec and held for 300 sec. Samples' thickness had been measured using the technique described in paragraph 2.4. The procedure was repeated for collagen samples that originate from 0.2, 0.3 and 0.4% collagen gels.

## 2.7 Estimation of Collagen Proportion

After mechanical testing, the ten 8mm-samples were weighed using a 4-digital balance (Precisa, Switzerland). The samples were desiccated for 5 days at 37°C. Collagen proportion was deduced based on the net weight of the initial hydrated samples and the net weight after desiccation.

## 2.8 Finite Element Modelling (FEM)

A FE model has been developed to simulate the *in vitro* testing of plastically compressed collagen gels using FEBio. FEBio is a nonlinear finite element program that was specifically developed to model and study biological tissues. The program allows for the implementation of an array of materials that may be assigned to soft tissues like collagen gels. It is an open source program that can be downloaded from [febio.org/](http://febio.org/).

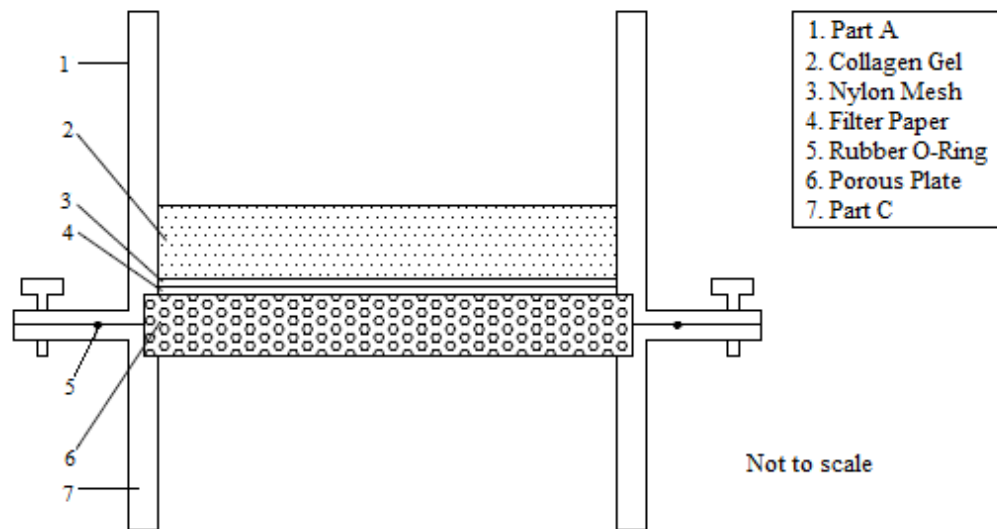


Figure 2.2.1: Experimental setup for collagen gel concentration. Part A and C have been bolted together. The rubber O-ring (5) prevents fluid leakage. A layer of nylon mesh (3) which is in direct contact with the gel and a layer of filter paper (4) mediate between the gel and the porous plate (6). Filter paper is permeable to water but not to collagen fibrils.

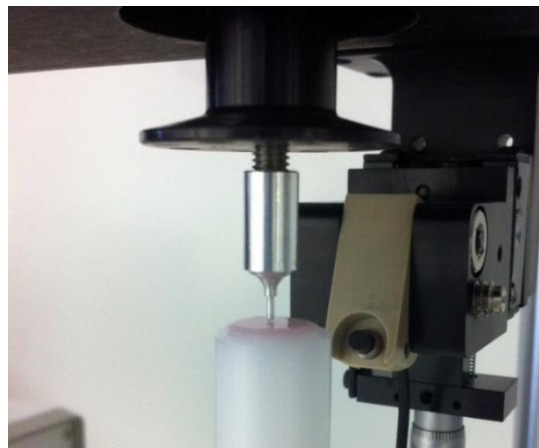


Figure 2.4.1: Apparatus for measuring the thickness of plastically compressed gels. The 1mm diameter aluminium tip perforates into the sample until it hits the sample's support which made of acetal.

A bespoke finite element model, one per each of the three groups, was developed to model the experiment of unconfined ramp hold compression. FE analysis was performed using FEBio (FEBio, Utah, US). The three parameters that change for each model were the sample height (thickness), the vertical displacement of the rigid body and the solid volume fraction.

### *Geometry*

The collagen gel was modelled as a symmetric quarter cylinder to reduce computational time. A diameter of 8mm was assigned to the cylinder (same as the diameter of the collagen samples). The height of the cylinder was as measured by the indentation technique described in paragraph 2.4. A rigid body assigned to a rigid interface was used to implement the compression.

### *Boundary Conditions (BCs)*

The BCs that were applied to the quarter cylinder can be listed as follows:

- a. The nodes of the bottom surface were constrained in the x, y and z direction
- b. The nodes of the top surface were constrained in the x and y direction
- c. Zero fluid pressure was assigned at the nodes of the circumferential boundary
- d. The nodes of the xz cross section were constrained in the y direction
- e. The nodes of the yz cross section were constrained in the x direction

The abrasive coat that was applied on top and bottom surfaces of the testing apparatus prevents any slippage providing a known boundary condition (BCs (a) and (b)). BC (c) allows for the outflow of fluid and the BCs (d) and (e) were applied to model the gel as a quarter cylinder.

### *Loading*

A prescribed vertical displacement was applied to the model to implement the compression. Vertical displacement was different for each of the three models depending on the sample thickness (calculated on the basis that the final strain should be 10% of the sample's thickness).

### *Mesh*

The butterfly meshing method was chosen as the most appropriate method to mesh the model. The 3,641-node model consists of 10 stacks and 3,000 elements.

### *Material*

Gel was modelled as a biphasic material with a neo-Hookean solid matrix. Initial values for Young's modulus, zero strain hydraulic permeability and non-linear permeability coefficient were set equal to 1kPa,  $10\text{mm}^4/\text{Ns}$  and 1, respectively. These values are subjected to change. A zero matrix Poisson ratio was assigned to the model due to low solid volume fraction. The relation that was used for permeability was that of Lai and Mow (1980) (5.3a). For small strains, Holmes and Mow permeability relation with strain (5.3b) may be reduced to Lai and Mow permeability by setting the parameter  $\kappa$  equal to zero. (Holmes and Mow 1990) Fluid and solid density were set equal to 1 to ignore gravity forces.

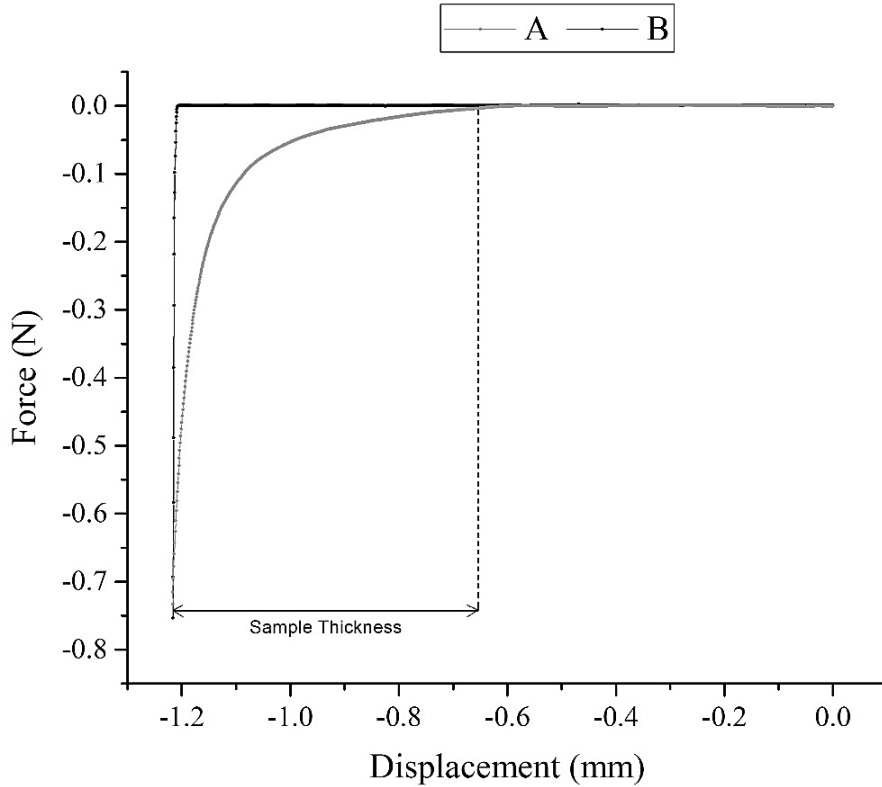


Figure 2.4.2: Indentation with (Graph A) and without sample (Graph B).

### Multi-Step Analysis

A multi-step analysis was performed to account for the ramp and the hold phase of the loading. A smaller time step was assigned for the ramp phase and the 10 first seconds of the hold phase as steep force response occurs (Table 5.8.1).

## 2.9 Parameter Optimisation

The predicted response upon loading based on the linear biphasic theory has to be fitted to the experimental force-time data (divided by 4 to equalize surface stress on the quarter cylindrical model to surface stress on the sample) to deduce material parameters. Curve-fitting was performed using the Levenberg-Marquardt (Levmar) algorithm. Levmar algorithm is an iterative method that finds a local minimum of the following function:

$$f(a) = \sum_{i=1}^n \{y_i - y(x_i, \vec{a})\}^2 \quad (2.9a)$$

where  $y_i$  array contains the experimental data,  $y(x_i, a)$  the theoretical prediction and the vector  $a$  contains the fitting parameters (zero-strain hydraulic permeability and Young's modulus). Eq. 2.9a expresses the sum of the squares of the deviation of the theoretical results from the

experimental results. Levmar algorithm interpolates by using the method of steepest descent and the Gauss-Newton iterative method. When the solution is located far from the experimental data, the algorithm behaves like a steepest descent; when the solution is located close to the experimental data, the algorithm behaves like a Gauss-Newton. [1]

## 2.10 Statistical Analysis

Significantly statistical differences for collagen concentration, thickness, peak force and tissue parameters among groups were compared by analysis of variance (ANOVA) followed by Tukey's test. Statistical analysis was performed using Origin<sup>®</sup>2015 (OriginLab, Graphing & Analysis).

## 2.11 Dynamic Loading

Specimens were also tested under dynamic loading and unconfined compression to find the relation of storage and loss moduli with frequency. In total, six 8mm-in-diameter self-compressed samples of 0.3% initial collagen concentration (collagen concentration before self-compression), obtained using the procedure described in paragraphs 2.1 and 2.2, were extracted using a hole punch. One sample was used for thickness measurement following the procedure described in paragraph 2.4. The rest five samples were placed on an impermeable flat support which was attached to a 250g load cell and compressed by a rigid cylinder. Both the lower support and the impermeable surface of the rigid cylinder were coated with wet and dry paper (1200 grit) to prevent gel slippage. The rigid cylinder was displacement controlled by a BOSE Electroforce<sup>®</sup> 3200 Test Instrument (BOSE, UK) accompanying by WinTest<sup>®</sup> software. A force filter of 10Hz was used to neglect large ambience frequencies.

Samples' surface was found by lowering the rigid cylinder until a force reading of 0.25g (stress equivalent to 48.8Pa) was achieved. Specimens were initially compressed by 5% and they immediately loaded with a sinusoidal displacement input of 0.1, 0.5, 1, 2, and 5Hz frequency. Wave amplitude (from peak to peak) was 10% of the sample's thickness. Phase lag  $\delta$  was deduced by fitting sinusoids (using the Levenberg-Marquardt numerical method) to both the strain input and the stress output to minimize the sum of squares. Data processing was performed using Origin<sup>®</sup>2015 (OriginLab, Graphing & Analysis).



# Results

## 3.1 Direct measures of gel characteristics

After 18 hours of confined self-compression, 0.2, 0.3 and 0.4% (w/v) collagen gels of 13mm thickness transformed to collagen sheets of 2.9, 3.2 and 3.6% (w/w) collagen of 0.45, 0.69 and 0.99 mm thickness, respectively (Figure 3.1.2 and 3.1.3). Results imply a ~10-fold increase in collagen density and induced strains of 92.3-96.5%.

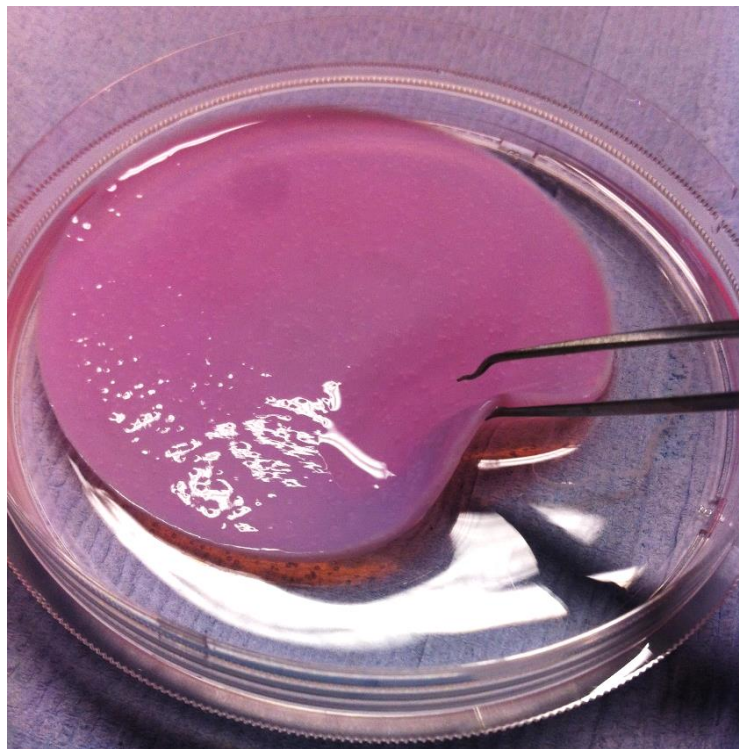


Figure 3.1.1: Collagen gel that has undergone confined self-compression for 18 hours- The collagenous sheet originates from a 0.4% collagen hydrogel that after 18 hours of compression under the force of gravity transformed to a thin and stable collagen sheet of 3.6% (w/w) collagen density.

Average peak surface stress for 2.9% collagen samples that were subjected to ramp hold experiment was 1,177Pa, slightly, but not significantly, larger than that of 3.2% collagen (1,120Pa) while peak stress for 3.6% collagen was estimated equal to 1,674Pa (Figure 3.1.4).

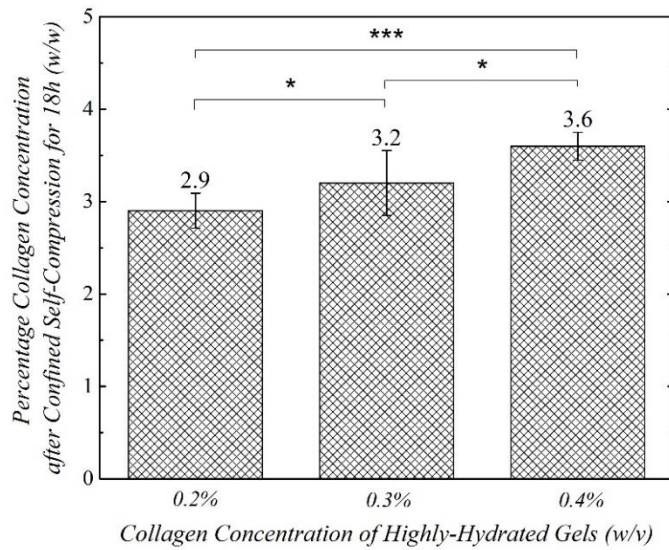


Figure 3.1.2: Percentage collagen proportion (w/w) of plastically compressed collagen gels that originate from highly-hydrated gels of different concentration. All 0.2, 0.3 and 0.4% (w/v) gels were left to self-compress for 18 hours at 20°C. Percentage collagen proportion is the average proportion as measured from 10 samples. Error bars indicate the standard deviation for each group, \*, \*\* and \*\*\* indicate  $p < 0.05$ , 0.01 and 0.001, respectively. A complete table with data for collagen proportion can be found in Appendix K.

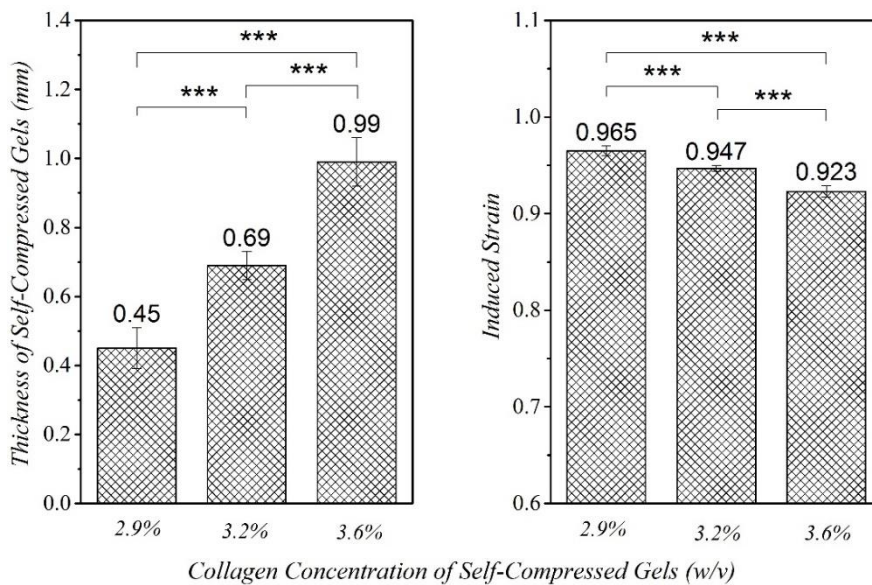


Figure 3.1.3: Thickness and percentage induced strain of plastically compressed collagen gels of different concentration. The initial thickness of pre-compressed gels was 13mm and the duration that all 0.2, 0.3 and 0.4% (w/v) gels were left to self-compress was 18 hours. Thickness is the average thickness of 5 measurements per each sample as measured by the technique described in paragraph 2.4. Error bars indicate the standard deviation for each group, \*, \*\* and \*\*\* indicate  $p < 0.05$ , 0.01 and 0.001, respectively. A complete table with data for thickness measurements can be found in Appendix L.

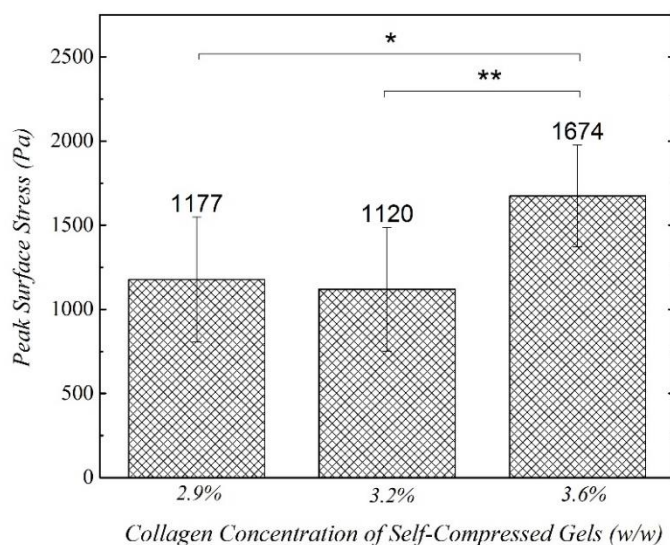


Figure 3.1.4: Peak surface stress for plastically compressed collagen gels of different concentration. Peak force is the average peak force per each group as obtained from the ramp-hold experiment described in paragraph 2.5. Error bars indicate the standard deviation for each group, \*, \*\* and \*\*\* indicate  $p < 0.05$ , 0.01 and 0.001, respectively. A complete table with data for thickness measurements can be found in Appendix M.

## 3.2 Surface Electron Microscopy (SEM)

SEM revealed the pores and collagen fibrils on collagen gel surface of the samples. Pore diameter of the fluid leaving surface of a 3.2% collagen sample was estimated equal to 0.88 $\mu$ m, greater than pore size of the top surface (0.68 $\mu$ m) while fibril diameter of a 2.9% collagen sample was estimated equal to 85nm ( $R^2 = 0.988$ ) (Appendix O).

## 3.3 Indirect Determination of Gel Characteristics

### 3.3.1 Model Prediction of Stress Relaxation

The FE model coupled with the optimization algorithm is able to accurately predict force response upon loading considering the complicate phenomena that the biphasic nature inserts into the problem. Only the hold phase of the experimental data was taken into account in the analysis. One fit for a 2.9% collagen sample was failed and was not included into the statistical analysis. The force response of that sample was quite low compared to the experimental force data obtained from the rest samples of the same group. Figure 3.3.1 presents the model fit for a sample of 2.9% collagen. Values for coefficient of determination  $R^2$  were greater than 0.90 in almost all the cases (26 out of 29 fits) indicating the reliability of the FE model (Appendix P).

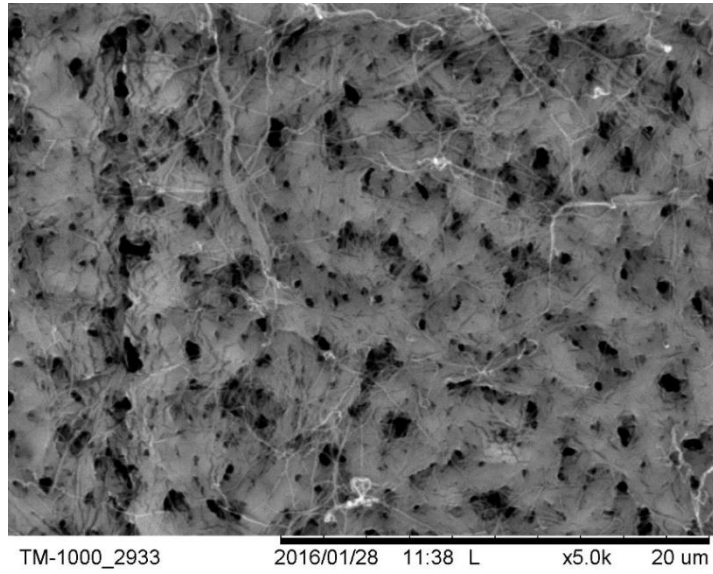


Figure 3.2.1: Scanning electron microscopy of the fluid leaving surface of a self-compressed gel of 3.2% collagen. Bar corresponds to 20 $\mu$ m (5,000 times magnification).

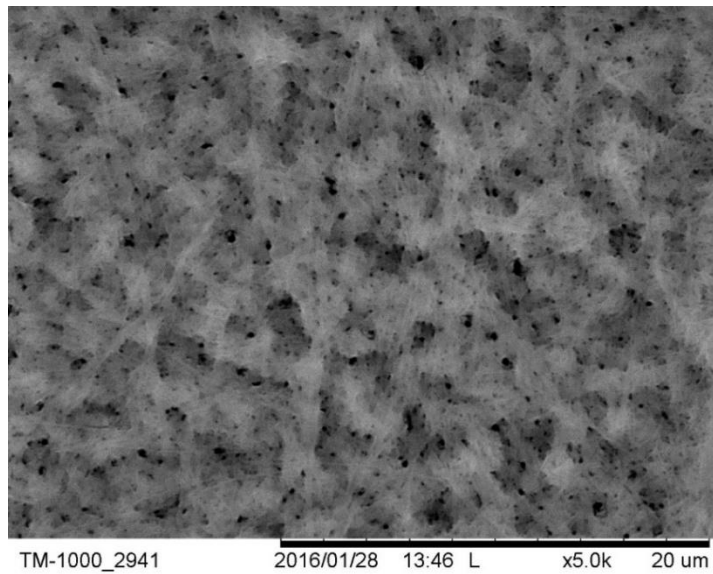


Figure 3.2.2: Scanning electron microscopy of the top surface of a self-compressed gel of 3.2% collagen. Bar corresponds to 20 $\mu$ m (5,000 times magnification).

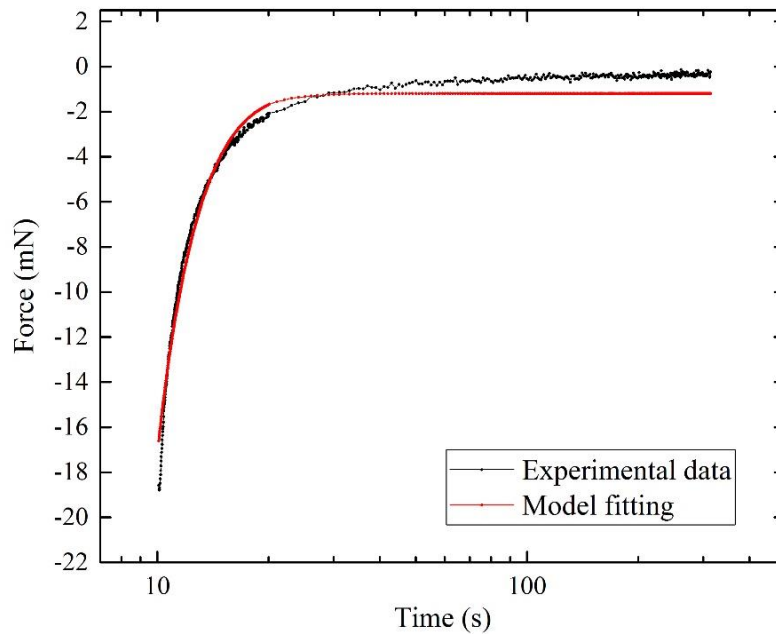


Figure 3.3.1: Curve fitting of the force response to ramp hold unconfined compression of a 2.9% collagen sample ( $R^2=0.976$ ). Experimental force data have been divided by four to be applied on the quarter cylinder.

### 3.3.2 Material Parameters

Indirect gel characteristics include Young's modulus, zero-strain hydraulic permeability and non-linear permeability coefficient. The latter expresses how quickly permeability decreases with increasing strain. Average Young's modulus of 2.9% collagen samples was found equal to 810Pa, slightly, but not significantly, larger than that of 3.2% collagen (755Pa), while Young's modulus of 3.6% collagen samples was found equal to 1,103Pa, significantly larger than that of 3.2% collagen (Figure 3.3.2). Zero-strain hydraulic permeability significantly decreased with increasing collagen content, from 51.4 mm<sup>4</sup>/Ns for 2.9% collagen samples to 31.8 and 21.2 mm<sup>4</sup>/Ns for 3.2 and 3.6% collagen, respectively (Figure 3.3.3), while non-linear permeability coefficient M was found equal to 11.9, 2.40 and 3.39, for 2.9, 3.2 and 3.6% collagen samples, respectively. Complete tables with results for material parameters can be found in Appendix R.

### 3.3.3 Frequency Dependence of Phase Lag and Dynamic Modulus

Dynamic mechanical analysis revealed a profound frequency dependence of phase lag ( $\delta$ ) and complex, storage and loss moduli (Figures 3.3.4, 3.3.5). A complete table with results for all specimens can be found in Appendix S.

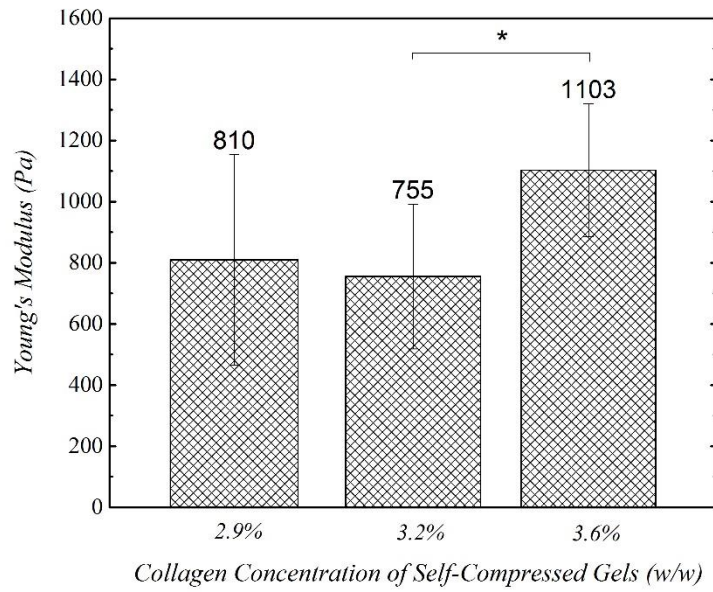


Figure 3.3.2: Young's modulus of plastically self-compressed collagen gels of different concentration. Young's modulus is the average Young's modulus per each group as obtained from parameter optimization. Error bars indicate the standard deviation for each group, \*, \*\* and \*\*\* indicate  $p < 0.05$ , 0.01 and 0.001, respectively.

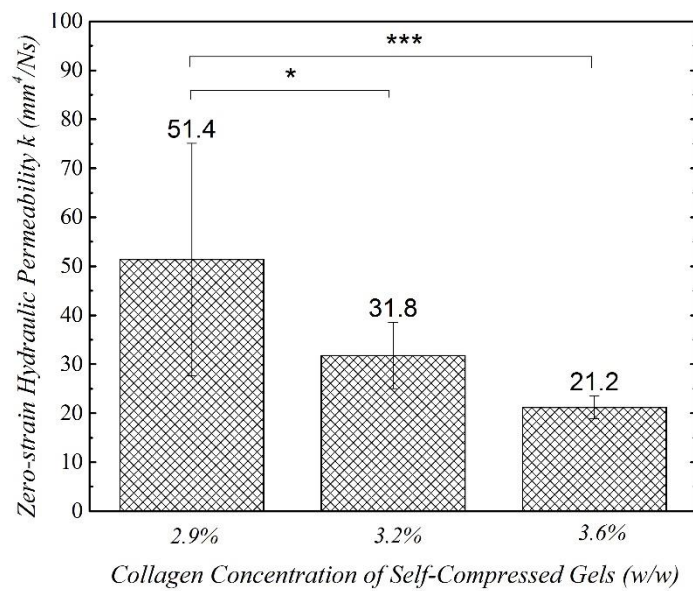


Figure 3.3.3: Zero-strain hydraulic permeability of plastically self-compressed collagen gels of different concentration. Permeability is the average permeability per each group as obtained from parameter optimization. Error bars indicate the standard deviation for each group, \*, \*\* and \*\*\* indicate  $p < 0.05$ , 0.01 and 0.001, respectively.

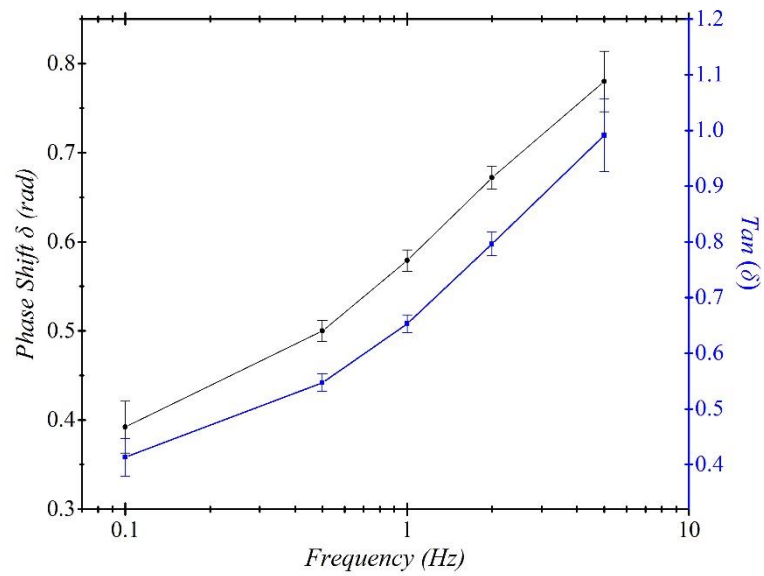


Figure 3.3.4: Phase lag ( $\delta$ ) dependence with frequency strain input for 3.2% (w/w) self-compressed collagen gels. Values for  $\delta$  are the average values taken from 5 samples. Bar errors correspond to standard variation. A Table with full data can be found in Appendix S.

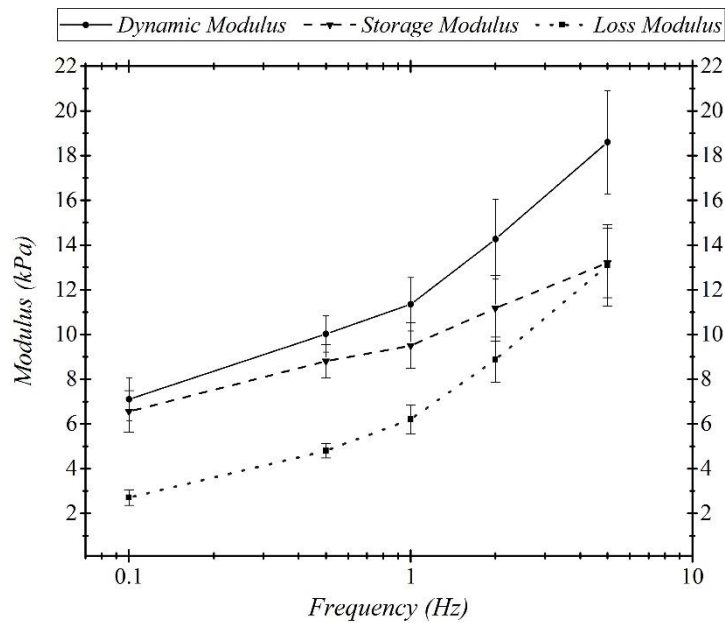


Figure 3.3.5: Complex, storage and loss moduli dependence with frequency strain input for 3.2% (w/w) self-compressed collagen gels. Values are the average values taken from 5 samples. Bar errors correspond to standard variation. A Table with full data can be found in Appendix S.



# Discussion

## 4.1 Collagen Gel Concentration

In this study, collagen gels were mechanically reinforced without using any cytotoxic method and without cellular activity which is highly uncontrollable. Gels were left to self-compress for 18 hours in a controllable manner to remove excessive interstitial fluid and to transform to structurally stable collagen sheets capable of sustaining their own weight.

However, one limitation of the methodology was the accidental formation of air bubbles inside the collagen gels which was the result of mixing during gel preparation. Since mixing was performed manually, the amounts of the trapped air and the density of air bubbles inside gels of different concentration were not identical. Air bubbles are stress raisers and potentially influence the mechanical response upon loading. In this study, no technique was adopted to impede or eliminate the formation of air bubbles. Further work could investigate the use of negative air pressure to remove the air bubbles during gelation. Another limitation of the study is that the method that was used to estimate collagen proportion, i.e. by desiccation for 5 days in 37°C does not guarantee utter dehydration; a maximum degree of dehydration could be achieved using a freeze drying technique which was not adopted in this study.

Gels of initial collagen density of 0.2, 0.3 and 0.4% (w/v) transformed to gels of 2.9, 3.2 and 3.6% (w/w) collagen, respectively. Hydrogels of initial 13mm thickness transformed to collagen sheets of 0.45, 0.69 and 0.99mm thickness while induced strain (compressive strain that was induced due to plastic self-compression) decreased with increasing collagen content.

Collagen gels were concentrated using confined compression which is a highly controllable method as fluid flow is limited in only one direction. On the contrary, Brown et al. (2005) and Neel et al. (2006) concentrated collagen gels using unconfined plastic compression and achieved a 40-fold increase in collagen density by the application of ~1.5kPa for 5 minutes. Final constructs' thickness ranged from 20-50µm. However, unconfined compression lacks control as fluid expulsion cannot be limited to only one direction. Light micrograph of the cross-section of a compressed collagen gel shows that collagen fibrils that are located closer to the fluid leaving surface are more concentrated than fibrils located far from the fluid leaving surface (Brown, et al. 2005) implying a steep axial strain gradient and different mechanical properties throughout the collagen bulk. In this study gels were left to self-compress for a large period of time to ensure that they reach equilibrium (i.e. null axial strain gradient).

## 4.2 Unconfined Ramp Hold Compression

Unconfined ramp-hold compression was considered a suitable experiment to obtain the mechanical properties of the self-compressed collagen gels as it is a simple experiment to perform to those thin samples. The wet and dry paper that was used to prevent gel slippage provides a clear boundary condition that was easily incorporated into the finite element model. The applied 10% compression on 0.5 to 1mm thick gels is quite challenging and requires very

accurate equipment. Force response was in the range of 1-2% of the load cell. Average peak surface stress ranged from 1.1 to 1.7kPa depending on collagen content. Interestingly, peak stress for collagen samples of 3.2% collagen was found slightly smaller than peak stress of 2.9% collagen samples. This discrepancy is attributed to experimental error. Busby et al. (2013) tested highly hydrated collagen gels in confined ramp hold compression. Peak stress ranged from 220-380Pa, around 5 times lower than peak stresses in this study. Peak surface stress depends on the rate of compression; material displays a stronger response for higher loading rates. Busby et al. compressed gels at a slower rate (0.5%/s) than in this study (1%/sec).

Collagen gels were modelled as biphasic materials with a hyperelastic neo-Hookean solid matrix and incorporating non-linear permeability (Lai and Mow, 1980). The neo-Hookean material that was chosen to model the solid matrix is a simple constitutive model which accounts for the potential large deformations that can be developed locally within the collagen matrix. Other hyperelastic models, with more parameters, may yield a better fit. Further, adding viscoelastic properties to the solid matrix (i.e. poroviscoelasticity) would result in a more realistic model as it may account for the known, time-dependent behaviour of the collagen fibres. Poisson's ratio effects were neglected by assigning a zero value and it was not inserted into the parameter optimisation. This value was chosen due to recent work on the nucleus pulposus (Farrell 2013), and also due to the very low solid fraction of the collagen. Farrell estimated the matrix Poisson's ratio of nucleus pulposus in the range of 0.1-0.2. This finding, combined with the facts that the nucleus pulposus consists of almost 20% collagen whilst self-compressed collagen gels are only 3-3.5% collagen justifies the approximation of zero Poisson's ratio that was adopted in this study. Nevertheless, in practice when Poisson's ratio and Young's modulus are fitted together (in one dimension) results are not reliable since an infinite number of parameter combinations yield identical results. Further, the Lai and Mow (1980) relationship for strain-dependent permeability is considered the simplest non-linear relation between permeability and strain as it utilises only one variable to describe the loss of permeability with compressive deformation. Again, more complex relationships incorporating more parameters may yield improved fits.

The strength of the model lies therefore on its simplicity. Only three parameters were fitted-Young's modulus, zero-strain hydraulic permeability and a non-linear permeability coefficient. Adding more parameters would probably result in better fit, however, when the number of parameters involved increases, it is possible that different combinations of values for material parameters would potentially result in equivalent fits, i.e. a non-uniqueness of solutions, and increase the possibility for convergence on a local minimum, not the global optimum. This would, in turn, lead to large standard deviations for the parameters fitted and reduce the interpretation capability of the model. Although only 3 key parameters were fitted, the fits yielded  $R^2$  values  $>0.90$  in almost all occasions, demonstrating that these three parameters account for over 90% of the experimental variability. Combined with the experimental difficulty and potential for experimental error, this finding is really encouraging.

Results indicate that compressive modulus of plastically self-compressed gels ranged from 755 to 1,103Pa. Previous studies have estimated the aggregate modulus of collagen hydrogels in the range of 900-1,200Pa (Busby, et al. 2013) and 318Pa (Knapp, et al. 1997) using confined ramp hold compression and biphasic theory. The moduli of the current study were around 3 times greater than that of highly hydrated gels found by Knapp et al. (1997) but similar to that obtained by Busby et al. (2013) for hyper-hydrated gels again. Knapp et al. compressed gels by 10% a rate of 0.08%/sec. This slow rate of compaction allows gels to dissipate a large

amount of their strain energy and present a low modulus. Busby et al., on the other hand, compressed gels at a higher rate in a confined manner and obtained higher values for modulus. It is speculated that the ~10-fold increase in collagen density that was achieved in the current work is not enough to observe differences in moduli between concentrated and highly-hydrated collagen gels.

The findings of this study also indicate loss of permeability with increasing collagen content. Zero-strain hydraulic permeability decreased from 51.4mm<sup>4</sup>/Ns for collagen samples of 2.9% collagen to 31.8mm<sup>4</sup>/Ns for collagen samples of 3.2% collagen and 21.2 mm<sup>4</sup>/Ns for 3.6% collagen. This result indicates that the model coupled with the optimisation algorithm is capable of detecting differences in hydraulic permeability among gels of different collagen proportion rendering the adopted method a reliable method to estimate material parameters of biphasic tissues. Busby et al. (2013) estimated zero-strain hydraulic permeability of hyper-hydrated collagen gels in the region of 75-170mm<sup>4</sup>/Ns, around 3 to 4-fold greater than zero-strain hydraulic permeability of self-compressed gels obtained in this study. This is as expected, since compaction of collagen gels reduces their porosity-permeability is dependent on porosity, the size and shape of the pores, the connectedness of the pores, and the tortuosity of the flow path. This is also an excellent result bearing in mind that Busby et al. (2013) tested gels under confined compression, with axial flow, whilst in this study gels were tested in unconfined compression with predominantly radial flow. The first estimate of permeability of collagen gels was made in 1997 by Knapp, et al. Darcy's permeability was estimated from creep testing and was found equal to 0.2 μm<sup>2</sup> (which is 20,000 mm<sup>4</sup>/Ns if fluid viscosity is considered 0.001 Pa·s), interestingly 100-250 times greater than that of highly hydrated collagen gels obtained by Busby et al. (2013) and 400-950 times greater than that of self-compressed collagen gels obtained in this study. However, Knapp et al. (1997) estimated permeability by fitting theoretical results obtained by solving the biphasic problem to experimental results obtained from long-time creep tests (5 hours) in confined compression. Their fits were dominated by the long tail of the relaxation phase while in this study, fits were dominated by the rate of stress relaxation immediately after the hold phase was reached.

Permeability is an important variable to consider when manufacturing a tissue equivalent as it is related to mechanical properties, cellular viability, activity, migration, oxygen flow, nutrient and waste diffusion. Some studies use Darcy's law to analyse experimental results and obtain permeability (Serpooshan et al., 2013). However, Darcy's law gives an estimate for tissue's permeability at a stage where the tissue is strained, i.e. at the end of compression phase, overestimating permeability. On the other hand, the Happel model that has been used to acquire values for permeability (Serpooshan et al., 2010, Serpooshan et al., 2011) provides estimates for permeability by making gross assumptions that do not account for the internal poromechanics that happen inside the biphasic material during loading. Biphasic theory provides values for the zero-strain hydraulic permeability of collagen gels, i.e. tissue's permeability before compression, by taking into account the stress, strain and fluid pressure gradients that are developed inside the tissue during loading.

Non-linear permeability coefficient was found equal to 12 for samples of 2.9% collagen, 2.4 for samples of 3.2% collagen and 3.4 for samples of 3.6% collagen. The permeability coefficient refers to the rate that permeability decreases with increasing compaction. According to Busby et al. (2013), permeability coefficient increased with increasing collagen content indicating that permeability of gels of greater collagen proportion decreases more rapidly than permeability of gels of lower collagen proportion. In this study, however, permeability

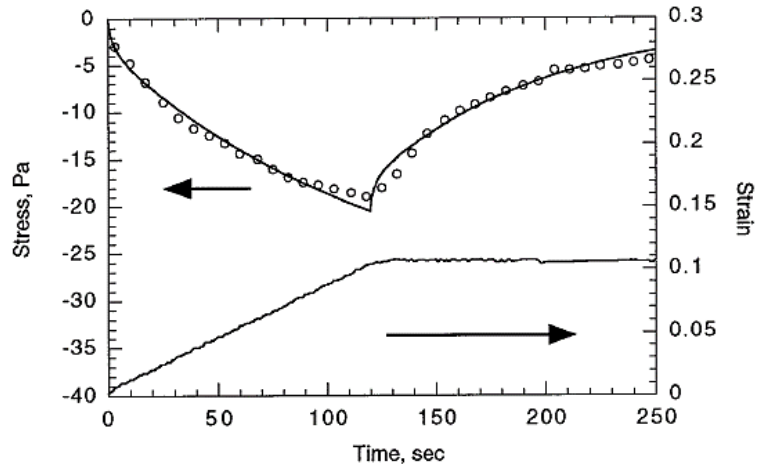


Figure 4.2.1: Confined compression ramp hold test results. Parameter estimates for collagen hydrogel in confined compression were obtained from fits of constant strain rate short-time ramp data. The gel was compressed to 10% strain at a constant strain rate over 120 s and then maintained at 10% strain ~actual strain trace shown. Theoretical prediction obtained by solving a form of biphasic theory developed by Barocas and Tranquillo (1997) was fitted to experimental results to obtain material parameters. Knapp, Barocas, Moon (1997)

coefficient for gels of 2.9% collagen was found significantly greater than permeability coefficient of gels of 3.2 and 3.6% collagen. The reason for this is unclear and further work is required in this area to ascertain how permeability varies with strain for gels of different starting porosity.

An estimate of the goodness of the fit and therefore the reliability of the FE model may be judged by coefficient of determination ( $R^2$ ). In this study, coefficient of determination for 26 out of 29 fits was estimated above 0.90 which clearly indicates that the FE model coupled with the optimisation algorithm fits the experimental data well. The goodness of fit is entirely in agreement with similar studies that have modelled collagen gels using biphasic theory (Busby et al. (2013), Knapp et al. (1997)). Figure 4.2.1 presents a model fit to experimental data obtained by confined ramp hold compression on highly hydrated collagen gels. (Knapp, Barocas and Moona 1997) In that study, a theoretical prediction of mechanical response acquired by solving a form of biphasic theory for anisotropic tissues that was developed by Barocas and Tranquillo (1997) was fitted to experimental data to obtain material parameters. Figure 4.2.2 shows a model fit of another research (an unpublished source). Authors tested highly hydrated collagen gels in confined ramp hold compression using biphasic theory. Linear biphasic theory was fitted to experimental results using a Nelder-Mead scheme to obtain the permeability-related ( $k_0$  and  $M$ ) parameters. In that study, samples were considered to have reached equilibrium and the fitting of the aggregate modulus  $H_A$  was based on only one experimental point, i.e. the last force reading at the end of the hold phase.

Today, there is a need for developing tools and protocols to study the mechanical behaviour of biphasic tissues. The main goal of the study is to develop and characterise plastically self-compressed collagen gels using biphasic theory. Biphasic theory accounts for the pressure gradients and the fluid flux that are developed due to the two-phase nature of gels and may influence cells in terms of growth, differentiation and general fate. Other theories (like viscoelasticity and hyperelasticity) totally ignore those phenomena. The number of studies that characterize collagen gels using biphasic theory is limited (Busby et al. (2013), Knapp et al. (1997)). To our knowledge, there is no study that characterizes concentrated collagen gels using biphasic theory; this study will provide literature values for these materials, identifying the

mechanical effect of expelling fluid from these constructs. A further novelty of this work is the modelling in unconfined compression. Previous modelling of soft tissue deformation has predominantly utilised confined compression, which is numerically simpler, but experimentally more complex. The recent development of FEBio to fit experimental data has facilitated this unique advancement.

The present study focuses on how the biphasic nature of gels influences the mechanical response upon loading. This is of utmost importance when cells are involved. Cells inside a medium that is modelled as a biphasic material experience much steeper stress and strain gradients than cells inside a viscoelastic medium due to (predictable) localised regions of high stress and strain. Consequently, hydrostatic stress, matrix stress/strain, and fluid flow, derived from biphasic analysis, will be important when studying the effects of mechanical loading upon cells (i.e. mechanobiology).

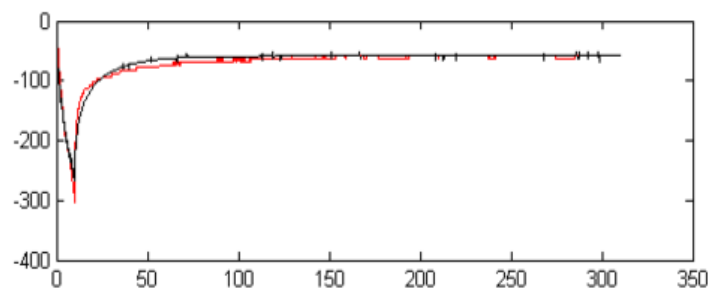


Figure 4.2.2: Confined ramp hold compression of a highly hydrated collagen gel. Experimental data have been fitted using linear biphasic theory and a Nelder-Mead scheme. Unpublished source.

### 4.3 Dynamic Mechanical Analysis (DMA)

The majority of the studies test collagen gels under shear oscillatory loading (conventional rheometry). Although shear rheometry may provide information about the storage and loss moduli, it is insufficient to fully characterize the mechanical behaviour of collagen gels. In shear, fluid and solid phase deform together, however, no information is given about the fluid flow with respect to the collagen matrix. (Knapp, Barocas and Moona 1997)

In this study, collagen samples were tested in compressive dynamic loading to explore the viscoelastic properties of self-compressed collagen gels. Samples were in a laterally confined state and strain input frequency was in the range of 0.1 to 5Hz. A higher frequency input would insert large errors into the analysis. Further, at physiological conditions, body tissues do not experience loading in high frequencies. Results revealed an increase of phase lag ( $\delta$ ), storage and loss moduli with increasing frequency input; samples displayed more solid-like behaviour for low frequencies and more fluid-like behaviour for higher frequencies. Gels' behaviour is analogue to a Maxwell fluid as both storage and loss moduli increase with frequency. On the contrary, native tissues have a frequency independent behaviour. The high fluid content (more than 96.5% (w/w)) is the main reason for the profound frequency dependence of self-compressed collagen gels. Further compression of collagen gels would result in a higher collagen density and possibly in a less profound frequency dependence. A question that also arises is would cell seeded self-compressed collagen gels display a frequency dependent behaviour?

## 4.4 Conclusion

In this study highly-hydrated collagen gels were left to self-compress for 18 hours in a confined manner in order to expel excessive fluid, to increase collagen density and therefore to increase mechanical properties. Collagen content increased around 10 times and ranged from 2.9-3.6% (w/v) collagen. Thickness of final constructs was in the region of 0.5 to 1mm indicating a 0.92 to 0.96 induced plastic strain due to self-compression. Collagen samples were tested in unconfined ramp hold compression and a finite element model (FE) was developed to analyse results. Material parameters were obtained by fitting a solution of the biphasic problem to experimental results. Compressive modulus was found in the range of 0.8-1.1kPa, many times lower than native tissues. Zero-strain hydraulic permeability was estimated in the range of 20-50 mm<sup>4</sup>/Ns, three to four times decreased than permeability of highly hydrated collagen gels (Busby, et al. 2013), but still thousands of times more permeable than tissues like articular cartilage (2.7 10<sup>-3</sup>mm<sup>4</sup>/Ns, Ateshian, et al., 1997) or nucleus pulposus (0.67 10<sup>-3</sup>mm<sup>4</sup>/Ns, Perie, et al., 2005). Zero-strain hydraulic permeability decreased with increasing collagen proportion indicating a good reliability of the FE model. Further, self-compressed collagen gels displayed a profound increase of phase lag ( $\delta$ ), storage and loss moduli with increasing frequency, in contrast to native tissues that display a flat response.

This research presents a completely controllable method to generate concentrated collagen gels that have the potential to be used in tissue engineering. The long-time self-compression and the laterally confined restriction allows samples to equilibrate. Although current final collagen constructs cannot substitute native tissue due to low mechanical properties, the methodology of confined compression that was followed may be evolved to achieve further increase in collagen density and mechanical properties even in the range of some body tissues.

In this work, mechanical behaviour of self-compressed collagen gels was studied using biphasic theory. In contrast to other theories, biphasic theory is the only theory that accounts for the interaction between fluid and solid phase, and the fluid pressure, stress and strain gradients that are developed due to this interaction. A further novelty of this study is the modelling in unconfined compression which is numerically more complex but experimentally simpler than confined compression. The current work may be used to develop more complex FE models of the biphasic tissue to explore the mechanical properties of concentrated collagen gels.

## 4.5 Future Challenges

The collagen concentration method via confined self-compression that was adopted in this research did not result in collagen constructs strong enough to substitute native tissue. A further compression of the gels in a confined controllable manner could potentially increase collagen density and therefore mechanical properties further, even in the range of body tissues. For instance, this could be achieved by using a rubber plug to impede any possible fluid flow through the upper surface (Figure 4.5.1). The rate of compression should be slow enough to allow tissue to equilibrate and eliminate final axial strain gradients. Nevertheless, mechanical testing of collagen sheets of smaller thickness (less than 0.5mm) is quite challenging.

The study forms an excellent basis from which more complicated constitutive behaviour can be applied to the FE model using a potentially hierarchical presentation of parameters to

the fitting algorithm to reduce large standard deviations when fitting in multiple parameter space. Future advances of the model could also include viscoelastic properties of the solid matrix (i.e. poroviscoelasticity) and a more complex permeability relation with strain. Clearly, further work is required to establish with certainty the nature of the relationship of permeability with strain.

Further, a question that arises from this work and could be explored in a future research is the mechanical behaviour of cell-seeded self-compressed collagen gels. Cells and GAGs have a dramatical impact on material parameters of the final collagen constructs, the degree of which depends on the type and number of cells, the culture period, the material properties of the collagen matrix, the external loading etc. Fibroblasts, for example, degrade and resynthesize the collagen matrix leading to fluctuations in mechanical properties with culture period. Further, cells are of larger diameter than pores of collagen lattice and therefore can decrease permeability by occluding them. They also interact with their substrate by exerting contractile forces that can align fibrils leading to anisotropy.

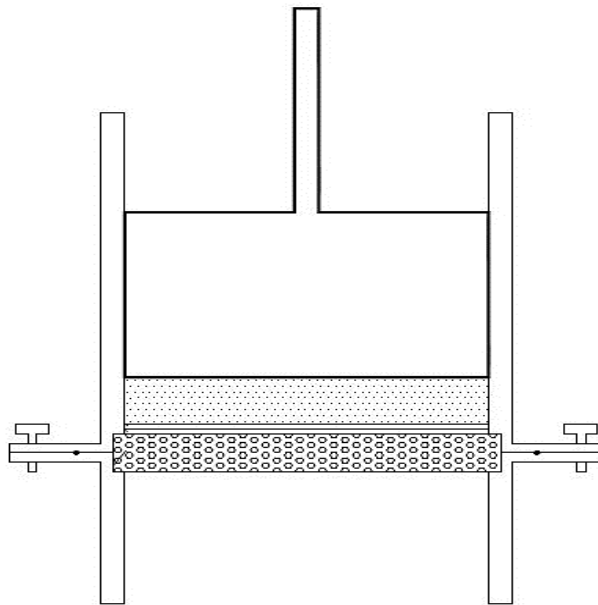


Figure 4.5.1: A future evolvement: Experimental set-up for concentration of collagen gels using confined compression.



## APPENDIX A

### Constitutive Equations and Mathematical Modelling of Biphasic Materials

The two sets of governing equations are the conservation of mass and linear momentum for the whole mixture. The conservation of mass for a porous material may be expressed by the following equation:

$$\nabla \cdot (\underline{v}^s + \underline{w}) = 0 \quad (5.1a)$$

where  $v^s$  is the velocity of the solid and  $w$  is the flux of the fluid relative to the solid. The interaction between fluid and solid may be expressed as momentum transfer from the fluid to the solid. Under quasi-static conditions, conservation of momentum may be reduced to the following relation:

$$\nabla \cdot \underline{\underline{\sigma}} + \rho \underline{b} = 0 \quad (5.1b)$$

where  $\sigma$  is the Cauchy stress tensor,  $\rho$  is the density of the mixture and  $b$  is the body force per mass. Since the mixture is porous the stress tensor may be expressed by the following relation:

$$\underline{\underline{\sigma}} = -p \underline{I} + \underline{\underline{\sigma}}^e \quad (5.1c)$$

where  $p$  the fluid pressure,  $I$  the identity tensor and  $\sigma^e$  the elastic stress developed in the solid matrix. This equation derives from the fact that stress which acting on the fluid is developed due to pore pressure in the pores whilst stress that acting on the solid matrix is caused by two factors: the elastic stress due to deformation of the solid network and the stress developed by hydrostatic fluid pressure acting from the fluid to the solid. Conservation of linear momentum states:

$$-\phi^f \nabla p + \rho^f \underline{b}^f + \underline{P} = 0 \quad (5.1d)$$

where  $\phi^f$  is the porosity,  $\rho^f$  is the apparent fluid density,  $b^f$  is the external body force per mass acting on the fluid and  $P$  is a vector with the linear momentum exchange between fluid and solid representing the frictional drag. Equation (5.1d) neglects viscous forces on the solid matrix.  $P$  can be related with the relative fluid flux  $w$  and the hydraulic permeability  $k$  with the following relation:

$$\underline{P} = -\phi^f \underline{k}^{-1} \cdot \underline{w} \quad (5.1e)$$

When Equation (5.1d) and (5.1e) are combined they produce Darcy's law:

$$\underline{w} = -\underline{k} \cdot (\nabla p - \rho_r^f \underline{b}^f) \quad (5.1f)$$

where  $\rho_f$  is true fluid density of the fluid which is related to the apparent density with the following relation:

$$\rho^f = \varphi^f \rho_T^f \quad (5.1g)$$

## APPENDIX B

### Poisson's Ratio Effect

Poisson's ratio is a material property which describes the relation between axial and lateral tissue expansion. In unconfined compression, Poisson's ratio is defined as:

$$\nu = -\frac{\varepsilon_{rr}}{\varepsilon_{zz}} \quad (5.2a)$$

where  $\varepsilon_{rr}$  is the radial strain and  $\varepsilon_{zz}$  the axial strain. An incompressible material has a Poisson's ratio of 0.5. A smaller value implies loss of volume with deformation. For most materials,  $\nu$  is independent on deformation and deformation rate, a material's constant. For biphasic materials there are two Poisson's ratios, the apparent one, which is the Poisson's ratio of the mixture, and the matrix Poisson's ratio, which is the Poisson's ratio of the solid matrix alone. The apparent Poisson's ratio may be determined in unconfined compression (with unrestrained radial displacement) using optical measurement techniques to estimate the lateral/radial deformation (e.g. Farrell 2013). Biphasic theory predicts a 0.5 value for the apparent Poisson's ratio at the start of the ramp phase due to the assumption of fluid incompressibility. However, this value is subjected to change due to fluid egress from the lateral boundary. In unconfined compression of a biphasic material, radial expansion would exceed the expansion that would have induced by matrix Poisson's ratio effect due to additional radial strains that are generated on the solid matrix by the moving fluid.

For poroelastic materials, it has been proposed that Poisson's ratio is linearly dependent on the magnitude of the applied axial strain. (Farrell 2013) Loss of voids (void collapse) inside the collagen network (which leads to increased solid volume fraction) due to increasing axial deformation results in an increased  $\nu$  as the material behaves more elastic. The same study suggests that Poisson's ratio increases with decreasing axial strain rate. The explanation that has been given for that phenomenon is that a slower ramp would allow for a faster and increased stress relaxation of the viscoelastic solid matrix leading to decreased strain energy, which in turn leads to decreased capability of the solid matrix to recoil. In the current study, due to the low solid volume fraction of the plastically compressed collagen gels (2.9 - 3.6% (w/w)), Poisson's ratio was assumed equal to zero.

## APPENDIX C

### Permeability

The first estimate of hydraulic permeability for collagen gels was made in 1997 by Knapp, et al. Permeability was estimated from creep in confined compression and results were analysed using biphasic theory. A finite element model was developed to analyse experimental results and an optimization process was used to fit theoretical results to experimental data. More recently, a similar study was performed by Busby et al. (2013) who used linear biphasic theory to study gel behaviour in stress relaxation and confined compression. By curve-fitting the numerical solution of the linear biphasic problem to force-time data acquired from the experiment, zero-strain hydraulic permeability was deduced.

Many studies have modelled biological porous tissues based on Darcy's law. (Bernich, Rubenstein and Bellin 1976) (Maroudas 1979) (Urban and Holm 1986) A study which refers to collagen gels is the one of Serpooshan et al. (2013)-by assigning suitable boundary conditions to Darcy's law, authors modified it to account for a two-layer model of a collagen gel loaded under confined plastic and self-compression. Using the modified Darcy's law, permeability was predicted based solely on the mass loss fraction which was defined experimentally.

However, Darcy's law gives no information about the stress-stain field that is developed inside the collagen when loaded. Biphasic theory of Mow (1980) and Holmes and Mow (1990), on the other hand, can precisely describe tissue response to external loading by taking into account the two-phase nature of collagen gels. During mechanical compaction, permeability decreases (strain dependency) as collagen fibrils get more densely packed and fluid finds greater resistance to exit the solid matrix. The relation between permeability and strain is described as a non-linear regression. Several models have been developed that relate permeability to stretch  $\lambda$  and/or tissue porosity  $\varphi$ :

$$\triangleright k = k_o e^{M(\lambda-1)} \quad (\text{Lai and Mow 1980}) \quad (5.3a)$$

$$\triangleright k = k_o \left( \frac{\lambda - 1 + \varphi_o}{\varphi_o} \right)^\kappa e^{\frac{1}{2}M(\lambda^2-1)} \quad (\text{Holmes and Mow 1990}) \quad (5.3b)$$

$$\triangleright k = k_o \left( \frac{\varphi}{\varphi_o} \right)^2 e^{M(\lambda-1)} \quad (\text{Argoudi and Shirazi-Adl 1996}) \quad (5.3c)$$

$$\triangleright k = k_o \left( \frac{\varphi}{\varphi_o} \right)^n \quad (\text{Riches, et al. 2002}) \quad (5.3d)$$

where  $k_o$  is the zero-strain hydraulic permeability,  $\varphi_o$  is the zero-strain porosity and  $M, n, \kappa$  are non-dimensional non-linear parameters describing the loss of permeability with strain. The suitability of each of the above-cited relations to describe loss of permeability is judged by fitting the theoretical prediction of each model to data obtained from the experiment.

Permeability of collagen gels has also been estimated by using Happel flow model. Happel model assumes flow through a random array of long rigid cylinders. In this model, it is assumed that the contribution of perpendicularly oriented fibrils to the global permeability accounts for two thirds while the rest one third is assigned to parallel fibrils. (Swartz and Fleury 2007) (Happel 1959)

$$k = \frac{2}{3}k_{\perp} + \frac{1}{3}k_{\parallel} \quad (5.3e)$$

According to Happel model permeability is a function of fibril radius  $a$  and solid volume fraction  $\sigma$ .

$$\triangleright k_{\perp} = \frac{\alpha^2}{8\sigma} \left\{ \ln\left(\frac{1}{\sigma}\right) - \frac{1-\sigma^2}{1+\sigma^2} \right\} \quad (5.3f)$$

$$\triangleright k_{\parallel} = \frac{\alpha^2}{8\sigma} \left\{ 2\ln\left(\frac{1}{\sigma}\right) + \sigma(4-\sigma) - 3 \right\} \quad (5.3g)$$

Serpooshan et al. (2010) used this model to predict permeability of collagen gels. However, Happel model does not take into account the drag forces that result from fluid-solid interaction and it does not give any information of the stress field, the fluid pressure gradients and the developed strains in the solid matrix. Further, a series of assumptions that Happel model makes may not be the case for plastically compressed collagen gels (e.g. uniform collagen density, randomly oriented fibrils).

## APPENDIX D

### Dynamic Mechanical Analysis (DMA)

Collagen gels may also be characterized in dynamic loading. The response of such materials depends on the frequency of the input (that can be stress or strain). The response to a sinusoidal stress/strain input may be a delayed sinusoidal strain/stress output. A complex dynamic modulus can be defined for such materials:

$$E = E' + iE'' \quad (5.4a)$$

where  $E'$  is known as the storage modulus (associated to the strain energy that has been stored in tissue) and  $E''$  is defined as the loss modulus (associated to the dissipated strain energy per cycle). The ratio of loss and storage modulus (5.4d) is a measure of how viscoelastic a material is.

$$E' = \frac{\sigma_o}{\epsilon_o} \cos \delta \quad (5.4b)$$

$$E'' = \frac{\sigma_o}{\epsilon_o} \sin \delta \quad (5.4c)$$

$$\frac{E''}{E'} = \tan \delta \quad (5.4d)$$

where  $\delta$  is the phase lag (delay) between stress and strain and  $\sigma_o$  and  $\epsilon_o$  are the stress and strain amplitudes, respectively.

For solids there is no delay between input and output ( $\delta = 0$ ) whilst for fluids  $\delta = \pi/2$ . Viscoelastic materials are somewhere in between ( $0 < \delta < \pi/2$ ). Collagen gels present a solid-like viscoelastic behaviour, typical for long polymers, as storage modulus is greater than loss modulus. (De Moraes, et al. 2012) However, for small strains (<15% (linear viscoelastic region)), it has been proposed that collagen gels behave more like a Maxwell fluid. (Chandran and Barocas 2004)

## APPENDIX E

### *Methodology*

#### Concentration of Collagen Hydrogels



Figure 5.5.1: Apparatus used for collagen solution casting (part A and B).

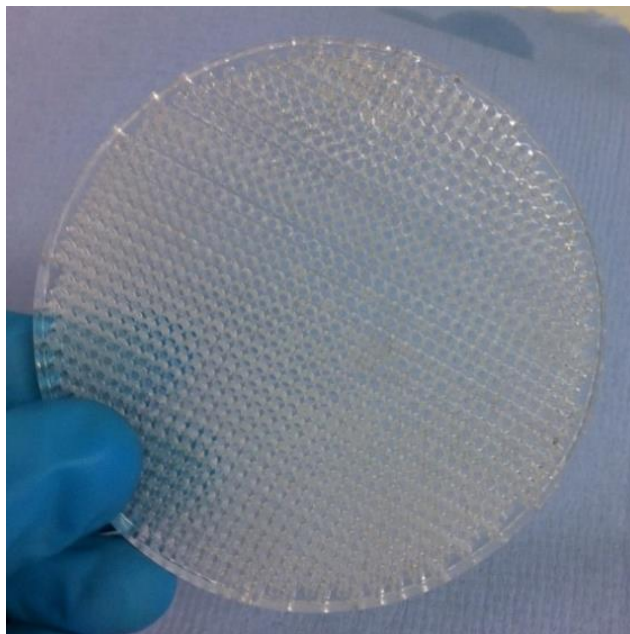


Figure 5.5.2: Acrylic porous plate (hole diameter 1mm, 25 holes/cm<sup>2</sup>) made with laser technique, 6mm thick.



Figure 5.5.3: Collagen gel concentration method. All the equipment has been turned upside down; the nylon mesh layer and the filter paper have been applied atop of the gel prior to the attachment of the porous plate and part C. The plug stays in place (due to large friction forces) when the apparatus is turned upside down. Gel was separated from the edges of the acrylic tube by using a scalpel.

# APPENDIX F

## *Methodology*

### Sampling

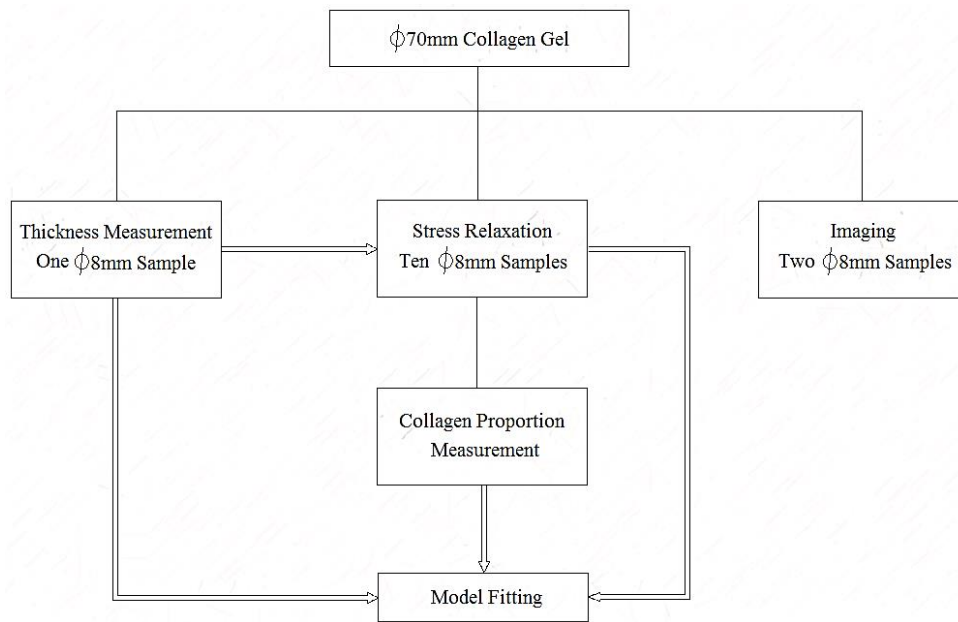


Figure 5.6.1: Diagram showing the procedure that was followed to characterize plastically compressed collagen gels. The procedure was repeated for collagen sheets that originate from 0.2, 0.3 and 0.4% collagen gels.

# APPENDIX G

## *Methodology*

### Unconfined Ramp Hold Compression

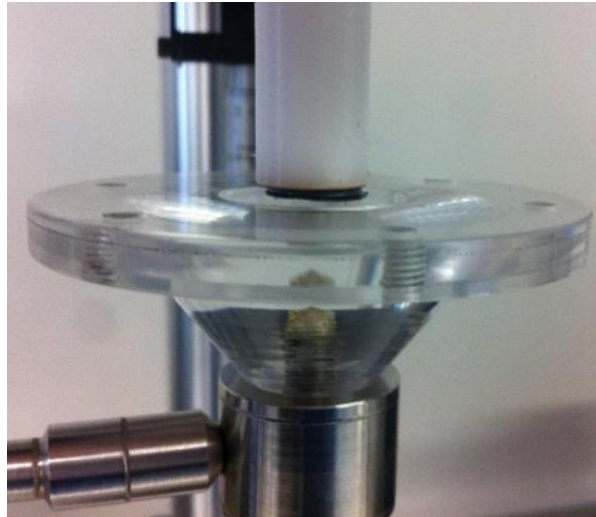


Figure 5.7.1: Experimental setup for unconfined compression of collagen gels.

# APPENDIX H

## *Methodology*

### Finite Element Modelling

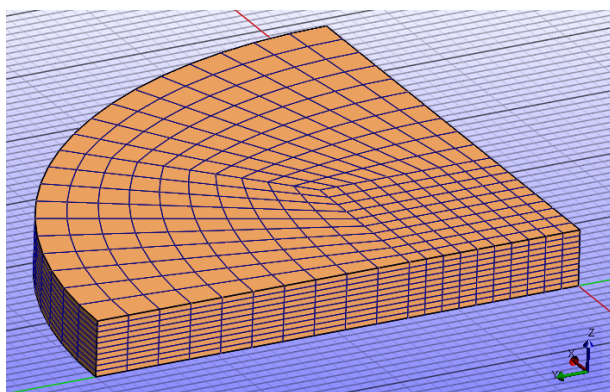


Figure 5.8.1: FE model of a plastically compressed collagen gel under unconfined ramp hold compression.

Step Name	Step Size (s)	Time Steps	Total Time (s)	Analysis Type
Ramp	0.01	1000	10	Transient
Hold-Start	0.01	1000	10	Transient
Hold	0.1	2900	290	Transient

Table 5.8.1: Time stepping parameters of the FE analysis.

# APPENDIX I

## *Methodology*

### FE algorithm

```
<?xml version="1.0" encoding="ISO-8859-1"?>
<febio_spec version="2.0">
  <Globals>
    <Constants>
      <T>0</T>
      <R>0</R>
      <Fc>0</Fc>
    </Constants>
  </Globals>
  <Material>
    <material id="1" name="Biphasic" type="biphasic">
      <phi0>
        !!!! Solid volume fraction of the collagen sample
        obtained from the experiment
      </phi0>
      <fluid_density>1</fluid_density>
      <solid type="neo-Hookean">
        <density>1</density>
        <E>0.001</E>
        <v>0</v>
      </solid>
      <permeability type="perm-Holmes-Mow">
        <perm>1</perm>
        <M>1</M>
        <alpha>0</alpha>
      </permeability>
    </material>
    <material id="2" name="Rigid1" type="rigid body">
      <density>1</density>
      <center_of_mass>
        !!!! The center of mass depends on the height of the
        sample obtained from the experiment
      </center_of_mass>
    </material>
  </Material>
  <Geometry>
    <Nodes>
      !!!! Node id of the Biphasic
    </Nodes>
    <Elements type="hex8" mat="1" elset="Part3">
      !!!! Element id of the Biphasic
    </Elements>
    <Elements type="hex8" mat="2" elset="Part4">
      !!!! Element id of the Rigid Body
    </Elements>
  </Geometry>
  <Boundary>
    <fix bc="xyz">
      !!!! Node id that have been fixed in x, y and z direction
    </fix>
    <fix bc="xy">
```

```

!!!! Node id that have fixed in x and y direction
</fix>
<fix bc="uvw">
!!!! Node is that have been fixed in Rx, Ry and Rz
direction
</fix>
<fix bc="y">
!!!! Node id that have been fixed in y direction
</fix>
<fix bc="x">
!!!! Node id that have been fixed in x direction
</fix>
<fix bc="p">
!!!! Node id that have been assigned with a zero fluid
pressure bc
</fix>
</Boundary>
<Contact>
  <contact type="rigid" name="Rigid_upper_interface">
!!!! Node id that have been assigned to the rigid
interface
  </contact>
</Contact>
<Constraints>
  <rigid_body mat="2">
    <fixed bc="x"/>
    <fixed bc="y"/>
    <fixed bc="Rx"/>
    <fixed bc="Ry"/>
    <fixed bc="Rz"/>
  </rigid_body>
  <rigid_body mat="2">
    <prescribed bc="z" lc="1">1</prescribed>
  </rigid_body>
</Constraints>
<LoadData>
  <loadcurve id="1" type="smooth">
!!!! Displacement-time data that correspond to
compressive strain
  </loadcurve>
</LoadData>
<Output>
  <plotfile type="febio">
    <var type="displacement"/>
    <var type="effective fluid pressure"/>
    <var type="fluid flux"/>
    <var type="fluid pressure"/>
    <var type="stress"/>
  </plotfile>
</Output>
<Step name="ramp">
  <Module type="biphasic"/>
  <Control>
    <time_steps>1000</time_steps>
    <step_size>0.01</step_size>
    <max_refs>15</max_refs>
    <max_ups>10</max_ups>
    <dtol>0.001</dtol>
    <etol>0.01</etol>
    <rtol>0</rtol>
    <ptol>0.01</ptol>
  </Control>
</Step>

```

```

        <lstol>0.9</lstol>
        <time_stepper>
            <dtmin>0.01</dtmin>
            <dtmax>1</dtmax>
            <max_retries>5</max_retries>
            <opt_iter>10</opt_iter>
        </time_stepper>
    </Control>
</Step>
<Step name="hold-start">
    <Module type="biphasic"/>
    <Control>
        <time_steps>1000</time_steps>
        <step_size>0.01</step_size>
        <max_refs>15</max_refs>
        <max_ups>10</max_ups>
        <dtol>0.001</dtol>
        <etol>0.01</etol>
        <rtol>0</rtol>
        <ptol>0.01</ptol>
        <lstol>0.9</lstol>
        <time_stepper>
            <dtmin>0.01</dtmin>
            <dtmax>1</dtmax>
            <max_retries>5</max_retries>
            <opt_iter>10</opt_iter>
        </time_stepper>
    </Control>
</Step>
<Step name="hold">
    <Module type="biphasic"/>
    <Control>
        <time_steps>2900</time_steps>
        <step_size>0.1</step_size>
        <max_refs>15</max_refs>
        <max_ups>10</max_ups>
        <dtol>0.001</dtol>
        <etol>0.01</etol>
        <rtol>0</rtol>
        <ptol>0.01</ptol>
        <lstol>0.9</lstol>
        <time_stepper>
            <dtmin>0.01</dtmin>
            <dtmax>10</dtmax>
            <max_retries>5</max_retries>
            <opt_iter>10</opt_iter>
        </time_stepper>
    </Control>
</Step>
</febio_spec>

```

# APPENDIX J

## *Methodology*

### Fitting algorithm

```
<?xml version="1.0" encoding="ISO-8859-1"?>
<febio_optimize>
<Model>
!!!! FEBio file name
</Model>
<Options type="constrained levmar">
  <obj_tol>0.001</obj_tol>
  <f_diff_scale>0.001</f_diff_scale>
</Options>
<Function>
  <fnc lc="1">
    !!!! Force-time data obtained from solving the biphasic
    problem
  </fnc>
</Function>
<Parameters>
  <param name="Biphasic.solid.E">0.001, 0.00001, 1</param>
  <param name="Biphasic.permeability.perm">1, 0.1, 1000 </param>
  <param name="Biphasic.permeability.M">1, 0.0000000001,
  100000000</param>
</Parameters>
<LoadData>
  <loadcurve id="1">
    !!!! Force-time data obtained from the experiment
  </loadcurve>
</LoadData>
</febio_optimize>
```

# APPENDIX K

## *Results*

### Collagen Proportion

Percentage collagen proportion (w/w) of samples that originate from 0.2, 0.3 and 0.4% (w/v) collagen gels. Group I, II and III correspond to collagen samples of 0.2, 0.3 and 0.4% gels, respectively.

<b>Sample</b>	<b>Group I</b>	<b>Group II</b>	<b>Group II</b>
A	2.71	3.88	3.63
B	2.85	3.00	3.46
C	3.16	2.93	3.44
D	2.93	2.82	3.92
E	2.98	2.96	3.62
F	3.23	3.62	3.52
G	2.58	3.05	3.70
H	3.00	3.51	3.50
I	2.93	3.28	3.60
J	2.92	3.35	3.46
<b>Average</b>	<b>2.93</b>	<b>3.24</b>	<b>3.58</b>
<b>STDEV</b>	<b>0.191</b>	<b>0.347</b>	<b>0.146</b>

Table 5.11.1: Percentage collagen proportion (w/w) of samples that originate from 0.2, 0.3 and 0.4% (w/v) collagen gels.

# APPENDIX L

## *Results*

### Thickness and Induced Strain

Thickness measurements of concentrated collagen samples. Average measurements were assumed as construct thickness.

<b>Indentation No</b>	<b>Thickness of 2.9% collagen sample (mm)</b>	<b>Thickness of 3.2% collagen sample (mm)</b>	<b>Thickness of 3.6% collagen sample (mm)</b>
i	0.38	0.63	1.0
ii	0.54	0.67	1.1
iii	0.41	0.72	1.0
iv	0.49	0.69	0.98
v	0.44	0.74	0.90
<b>Average</b>	<b>0.45</b>	<b>0.69</b>	<b>0.99</b>
<b>STDEV</b>	<b>0.064</b>	<b>0.042</b>	<b>0.056</b>

Table 5.12.1: Thickness measurements of concentrated collagen samples.

# APPENDIX M

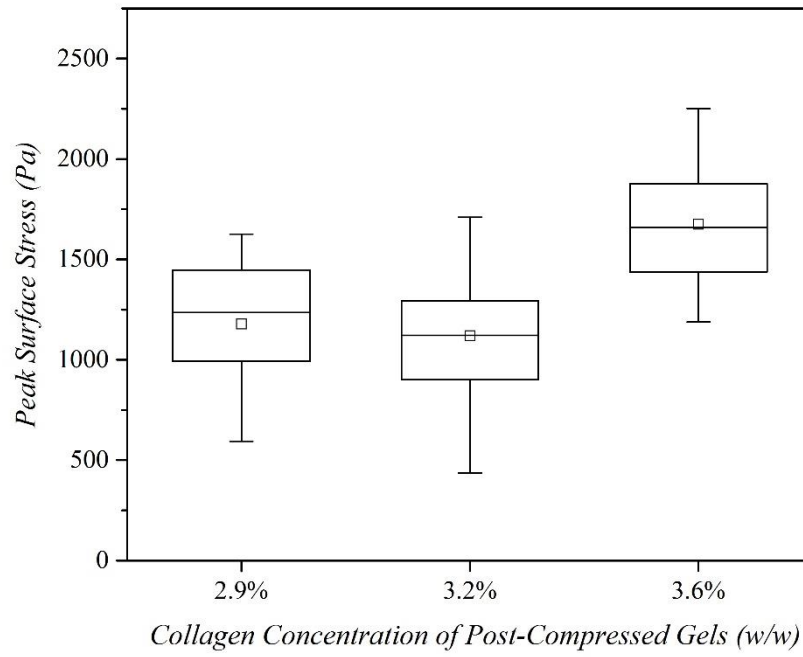
## *Results*

### Peak Stress

Peak stress of 2.9, 3.2 and 3.6% collagen samples as obtained from ramp-hold compression tests.

Sample	Peak Surface Stress (Pa)		
	2.9% Collagen	3.2% Collagen	3.6% Collagen
A	1523	1103	1585
B	1380	958	2252
C	1162	1564	1656
D	1625	1710	1390
E	992	901	1189
F	594	832	1751
G	1448	1295	1941
H	1235	1141	1665
I	-	1260	1876
J	637	437	1438
<b>Average</b>	<b>1177</b>	<b>1120</b>	<b>1674</b>
<b>STDEV</b>	<b>372</b>	<b>368</b>	<b>304</b>

Table 5.13.1: Peak surface stress of 2.9, 3.2 and 3.6% collagen samples.



Box Chart 5.13.1: Peak surface stress for 2.9, 3.2 and 3.6% collagen samples. □ implies the mean value.

# APPENDIX N

## *Results*

### Scanning Electron Microscopy (SEM)

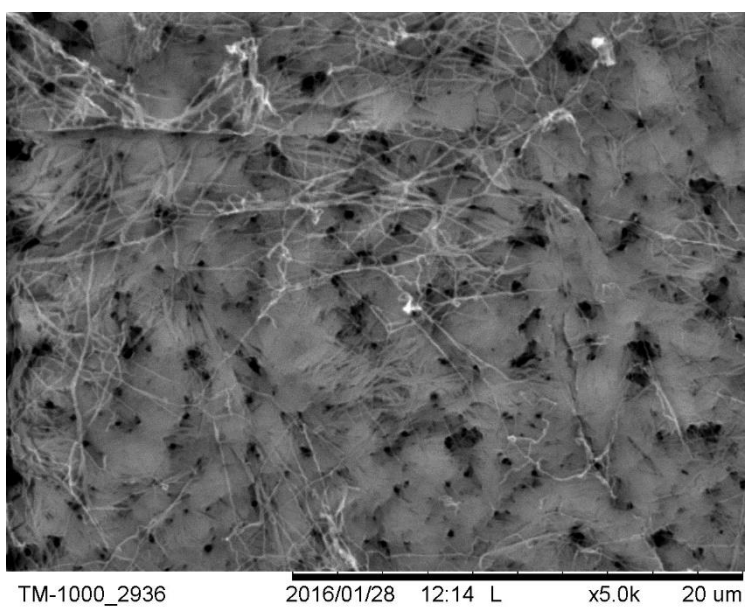


Figure 5.14.1: Scanning electron microscopy of the fluid leaving surface of a self-compressed gel of 3.2% collagen. Bar corresponds to 20 $\mu$ m (5,000 times magnification).

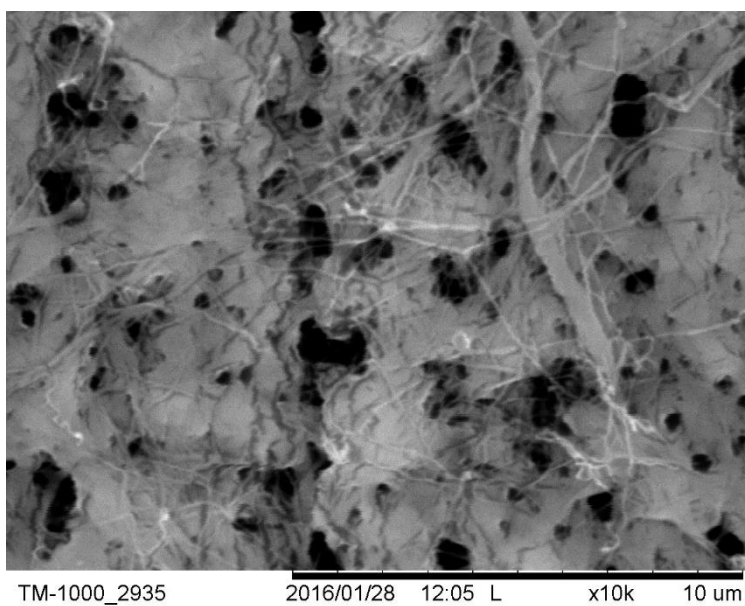


Figure 5.14.2: Scanning electron microscopy of the fluid leaving surface of a self-compressed gel of 3.2% collagen. Bar corresponds to 10 $\mu$ m (10,000 times magnification).

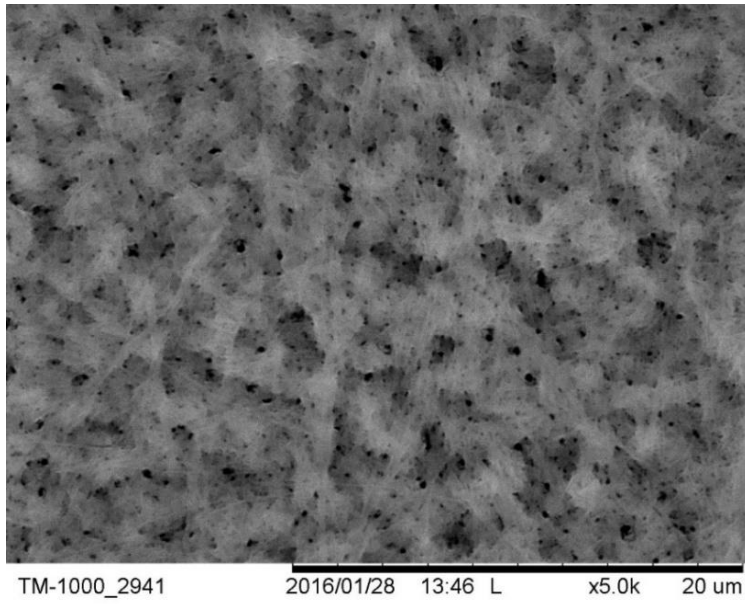


Figure 5.14.3: Scanning electron microscopy of the top surface of a self-compressed gel of 3.2% collagen. Bar corresponds to 20 $\mu$ m (5,000 times magnification).

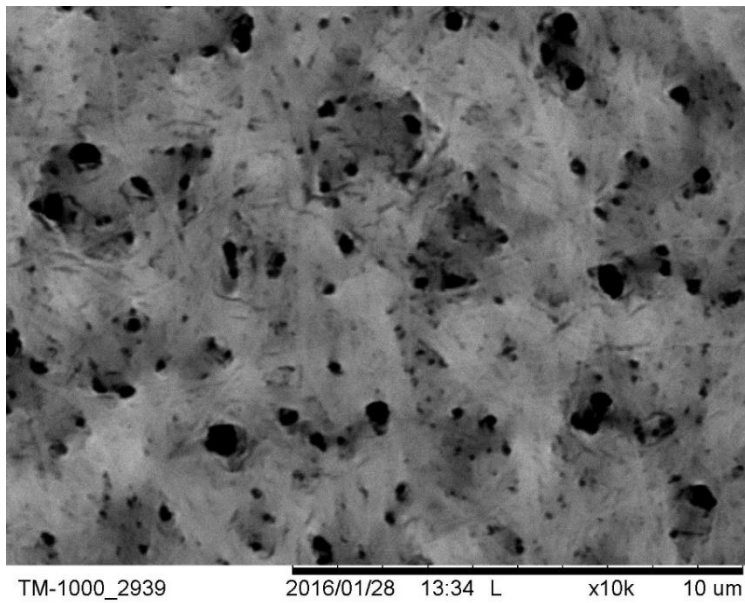


Figure 5.14.4: Scanning electron microscopy of the top surface of a self-compressed gel of 3.2% collagen. Bar corresponds to 10 $\mu$ m (10,000 times magnification).

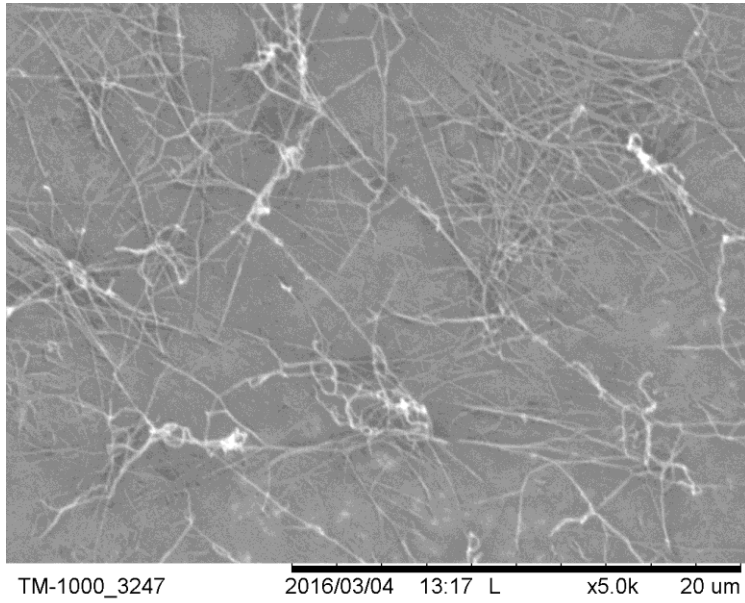


Figure 5.14.5: Scanning electron microscopy of the fluid leaving surface of a self-compressed gel of 2.9% collagen showing the superficial collagen fibrils. Bar corresponds to 20 $\mu$ m (5,000 times magnification).

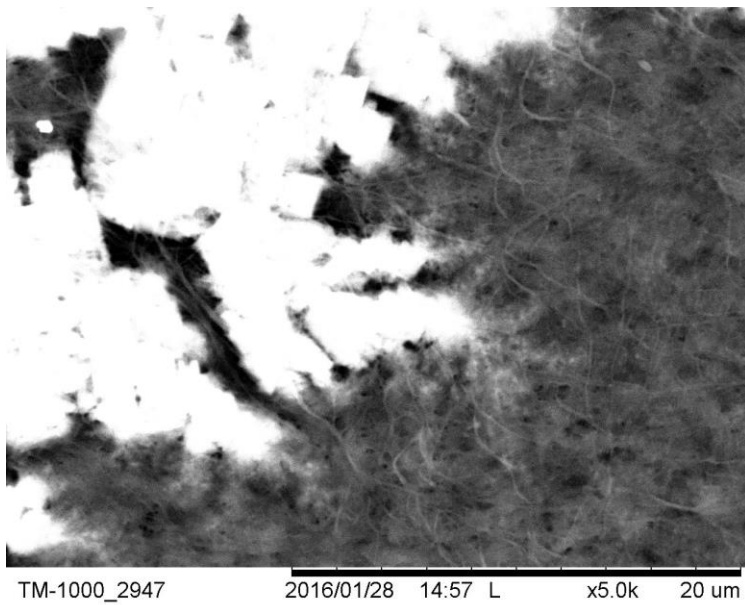


Figure 5.14.6: Scanning electron microscopy of the fluid leaving surface of a self-compressed gel of 3.6% collagen. Bright area is air trapped inside the collagen matrix. Bar corresponds to 20 $\mu$ m (5,000 times magnification).

# APPENDIX O

## Results

### Image Processing

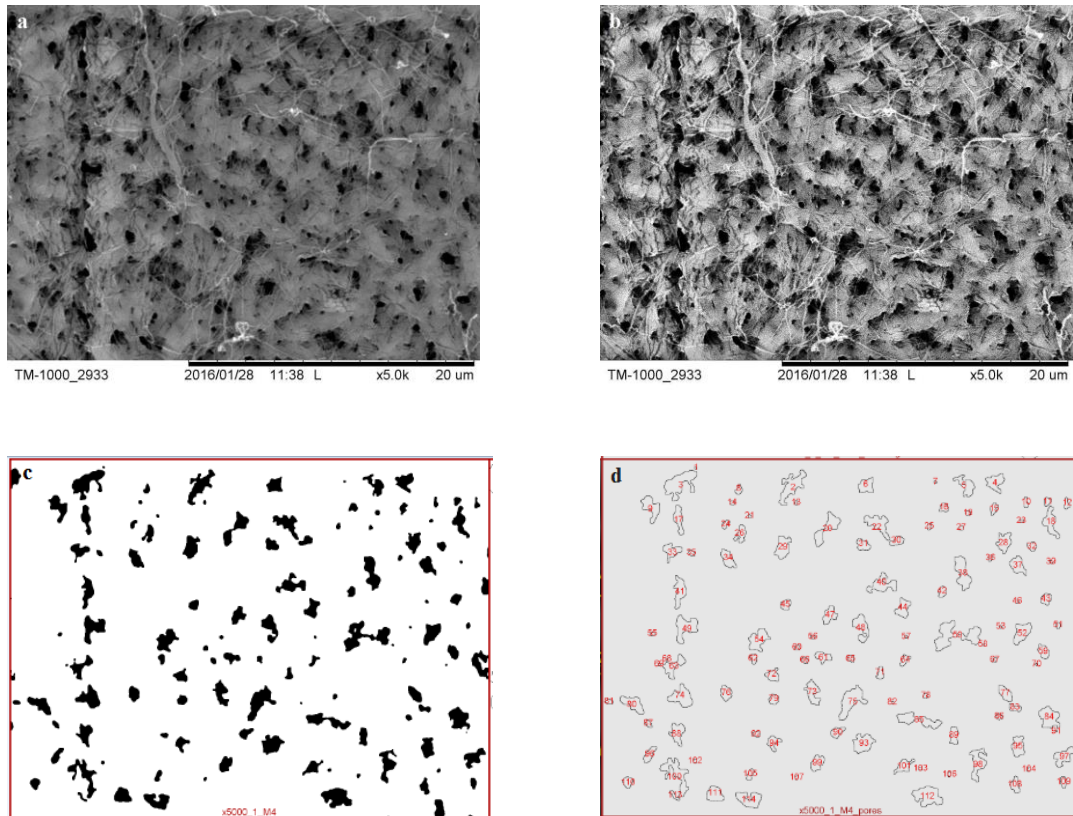


Figure 5.15.1: Image processing of the fluid leaving surface of a 3.2% collagen sample. (a) Original SEM image, (b) SEM image after contrast enhancement, (c) transition to black and white colour scale and (d) image processing for pore size estimation. Image processing was performed using ImageJ.

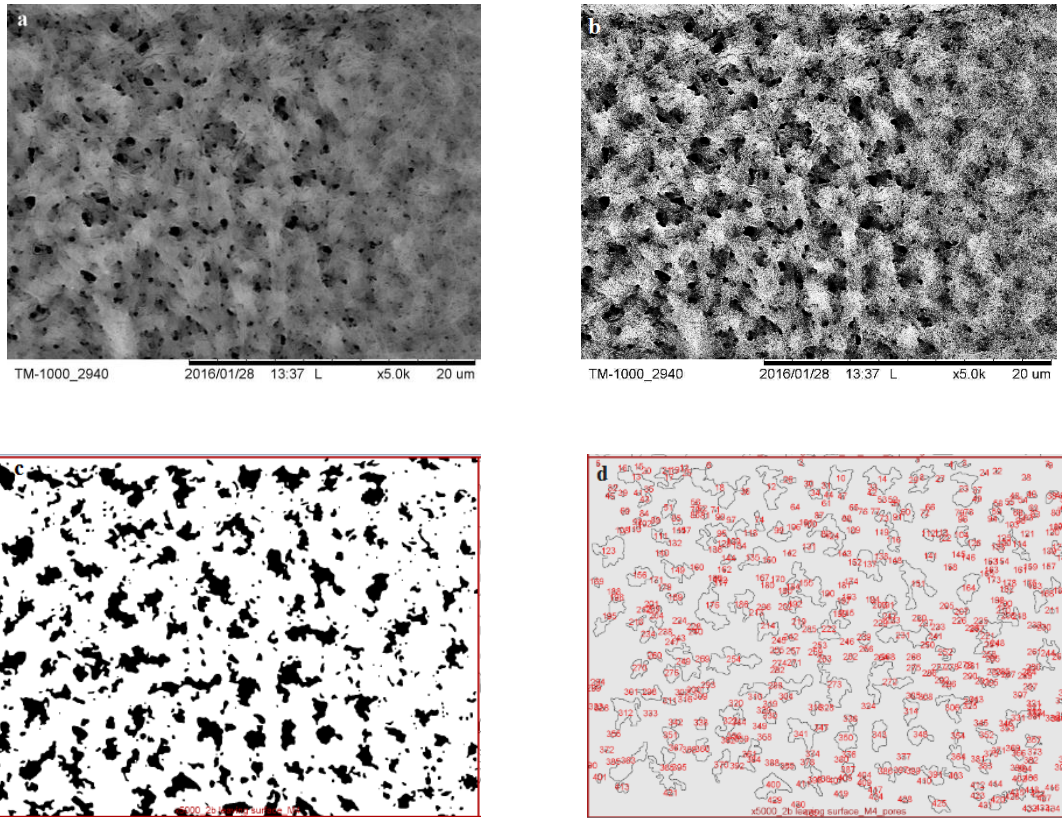


Figure 5.15.2: Image processing of the top surface of a 3.2% collagen sample. (a) Original SEM image, (b) SEM image after contrast enhancement, (c) transition to black and white colour scale and (d) image processing for pore size estimation. Image processing was performed using ImageJ.

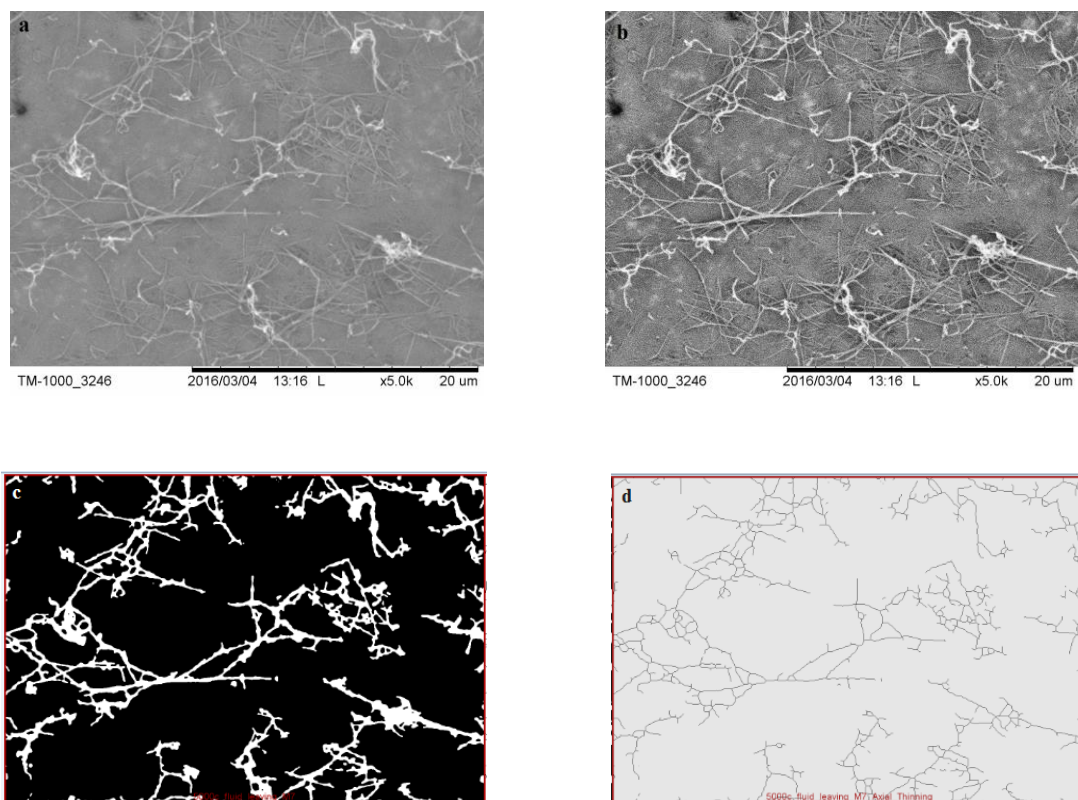


Figure 5.15.3: Image processing of the surface fibrils of a 2.9% collagen sample. (a) Original SEM image, (b) SEM image after contrast enhancement, (c) transition to black and white colour scale and (d) image processing for fibril diameter estimation. Image processing was performed using ImageJ.

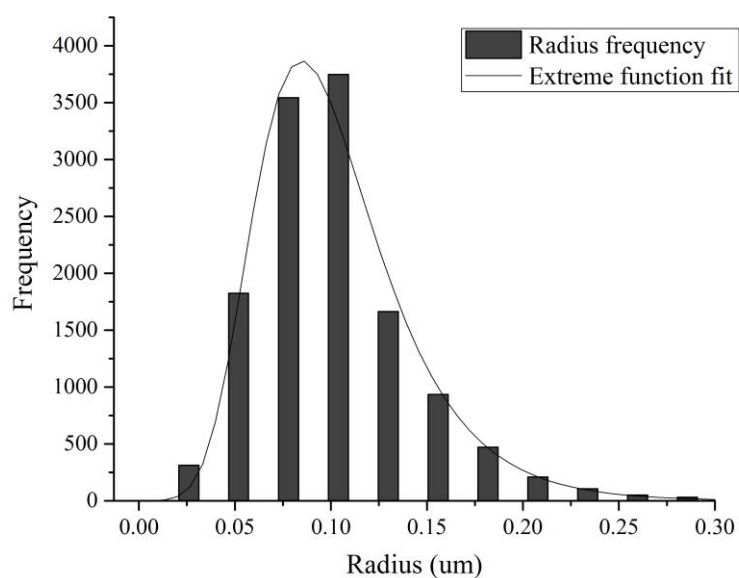


Figure 5.15.4: Fit of a histogram showing the frequency of different values for fibril radius. The histogram was fitted with the Extreme peak function to estimate the fibril diameter. Fitting was performed using Origin®2015 (OriginLab, Graphing & Analysis).

Formula of the Extreme function:

$$y = y_0 + Ae^{1-z-e^{-z}} \quad (5.15a)$$

$$z = \frac{x - x_c}{w}$$

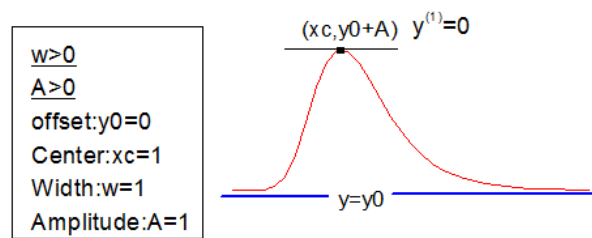


Figure 5.15.5: Parameters of the Extreme function. Source: OriginLab.

# APPENDIX P

## Results

### Model Fitting

To illustrate the typical model prediction, a good and a bad fit per each 2.9, 3.2 and 3.6% collagen gel are presented.

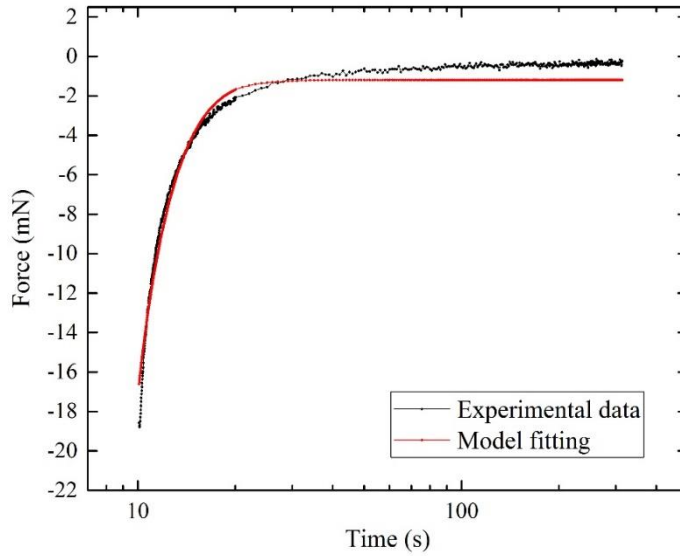


Figure 5.16.1: Curve fitting of the force response to ramp hold unconfined compression of a 2.9% collagen sample ( $R^2=0.976$ ). Experimental force data have been divided by four to be applied on the quarter cylinder.

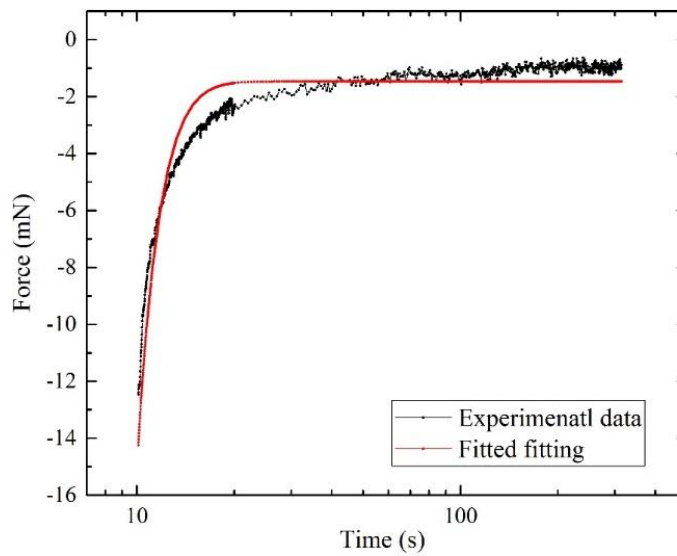


Figure 5.16.2: Curve fitting of the force response to ramp-hold unconfined compression of a 2.9% collagen sample ( $R^2=0.869$ ). Experimental force data have been divided by four to be applied on the quarter cylinder.

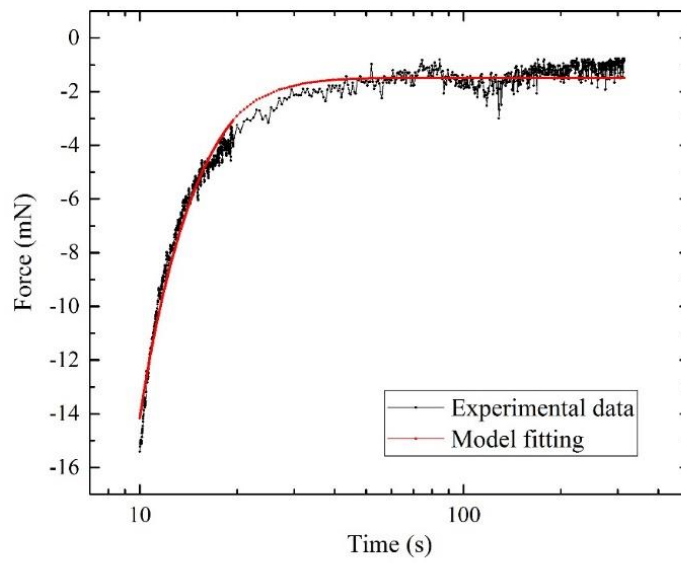


Figure 5.16.3: Curve fitting of the force response to ramp-hold unconfined compression of a 3.2% collagen sample ( $R^2=0.981$ ). Experimental force data have been divided by four to be applied on the quarter cylinder.

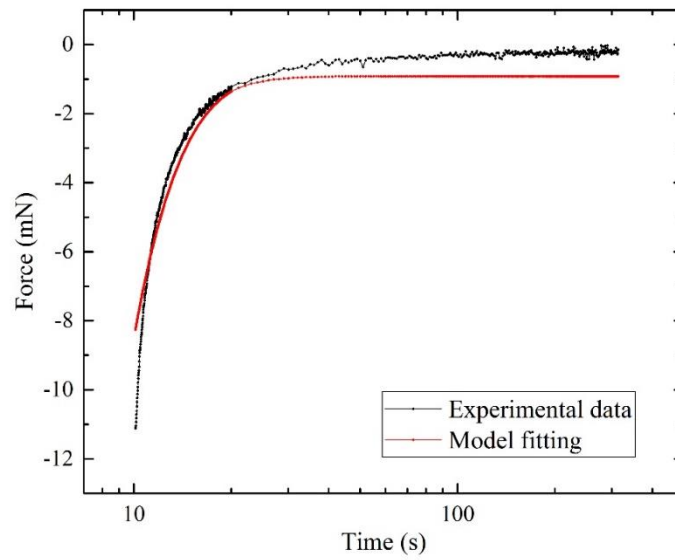


Figure 5.16.4: Curve fitting of the force response to ramp-hold unconfined compression of a 3.2% collagen sample ( $R^2=0.938$ ). Experimental force data have been divided by four to be applied on the quarter cylinder.

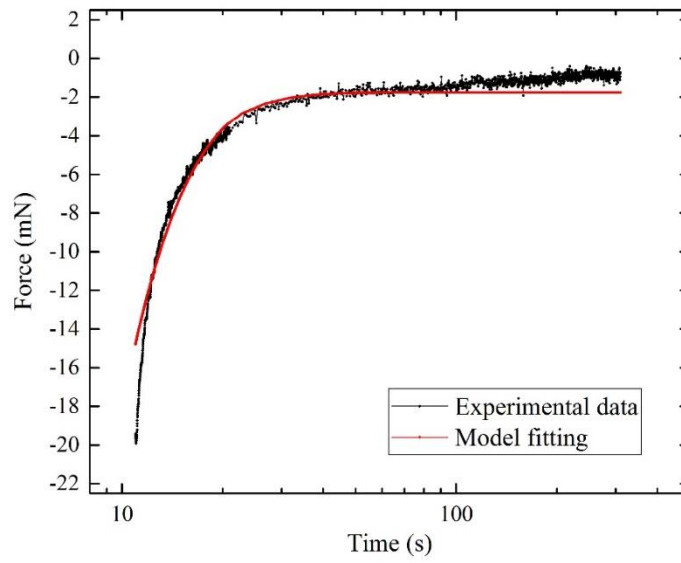


Figure 5.16.5: Curve fitting of the force response to ramp-hold unconfined compression of a 3.6% collagen sample ( $R^2=0.954$ ). Experimental force data have been divided by four to be applied on the quarter cylinder.

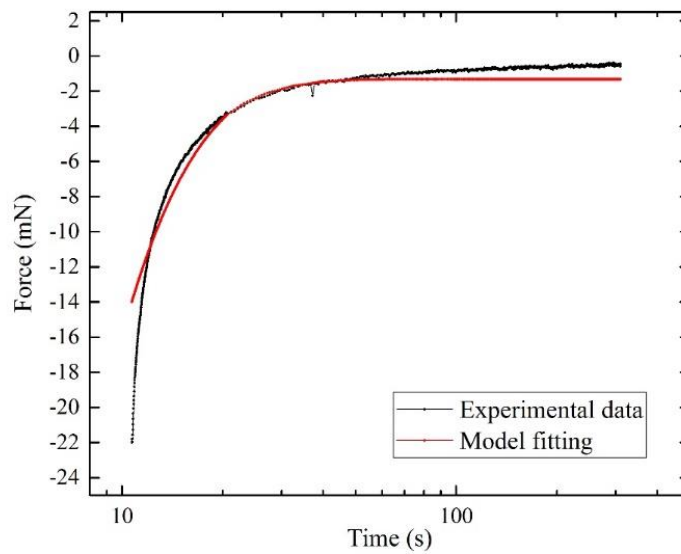


Figure 5.16.6: Curve fitting of the force response to ramp-hold unconfined compression of a 3.6% collagen sample ( $R^2=0.929$ ). Experimental force data have been divided by four to be applied on the quarter cylinder.

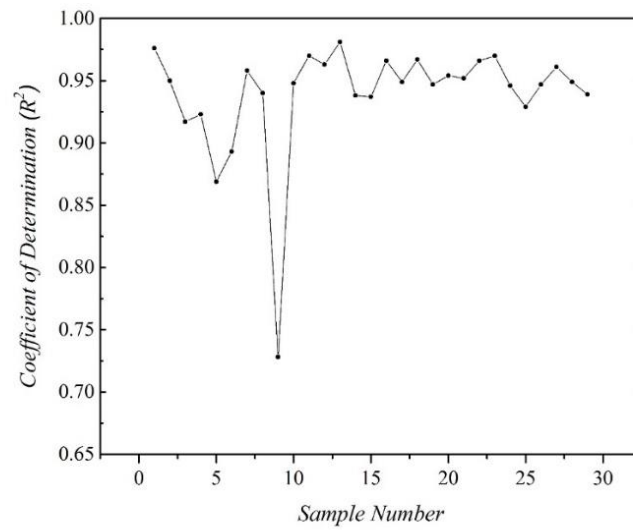


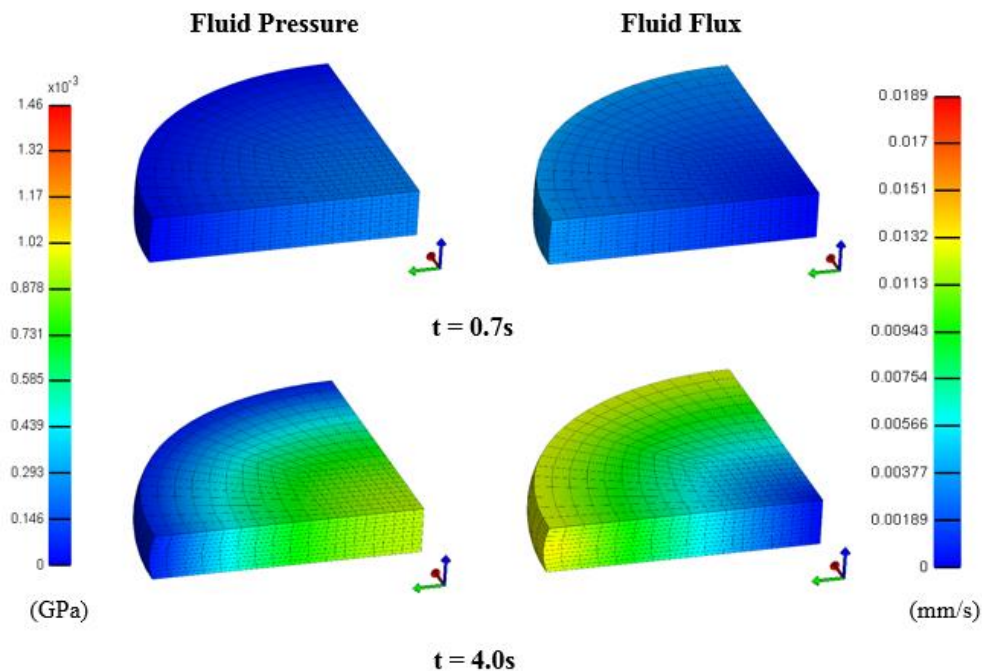
Figure 5.16.7: Coefficient of determination ( $R^2$ ) for the fits of stress relaxation of collagen gels of different concentration. Coefficient of determination is a commonly accepted indicator of the goodness of the fit.

# APPENDIX Q

## Model Prediction of Internal Poromechanics

The liquid phase (or the interstitial fluid) is incompressible and thus it must maintain constant volume during deformation. In unconfined compression, the solid phase is radially strained by the fluid as the fluid should deform radially maintaining constant volume. Tensile radial elastic stresses are generated on the solid matrix as a result of the viscous drag which gives rise to additional compressive axial stress. These tensile radial stresses are over and above those that would have been generated by Poisson's ratio effect only, and are balanced by a rise in fluid pressure. Initially, steep radial fluid pressure, radial stress and radial strain gradients are generated at the lateral boundary (free draining surface). Fluid egress through this boundary lessens all the gradients leading to a gradual radial recoil. At equilibrium, all gradients have been annihilated and the deformation of the tissue is governed by Poisson's ratio and Young's modulus of the solid phase.

Figure 5.17.1 shows the radial fluid pressure and the radial fluid flux of a 3.2% (w/w) collagen gel. Simulation is based on the material parameters that were obtained from curve fitting of the numerical solution of biphasic theory to experimental results.



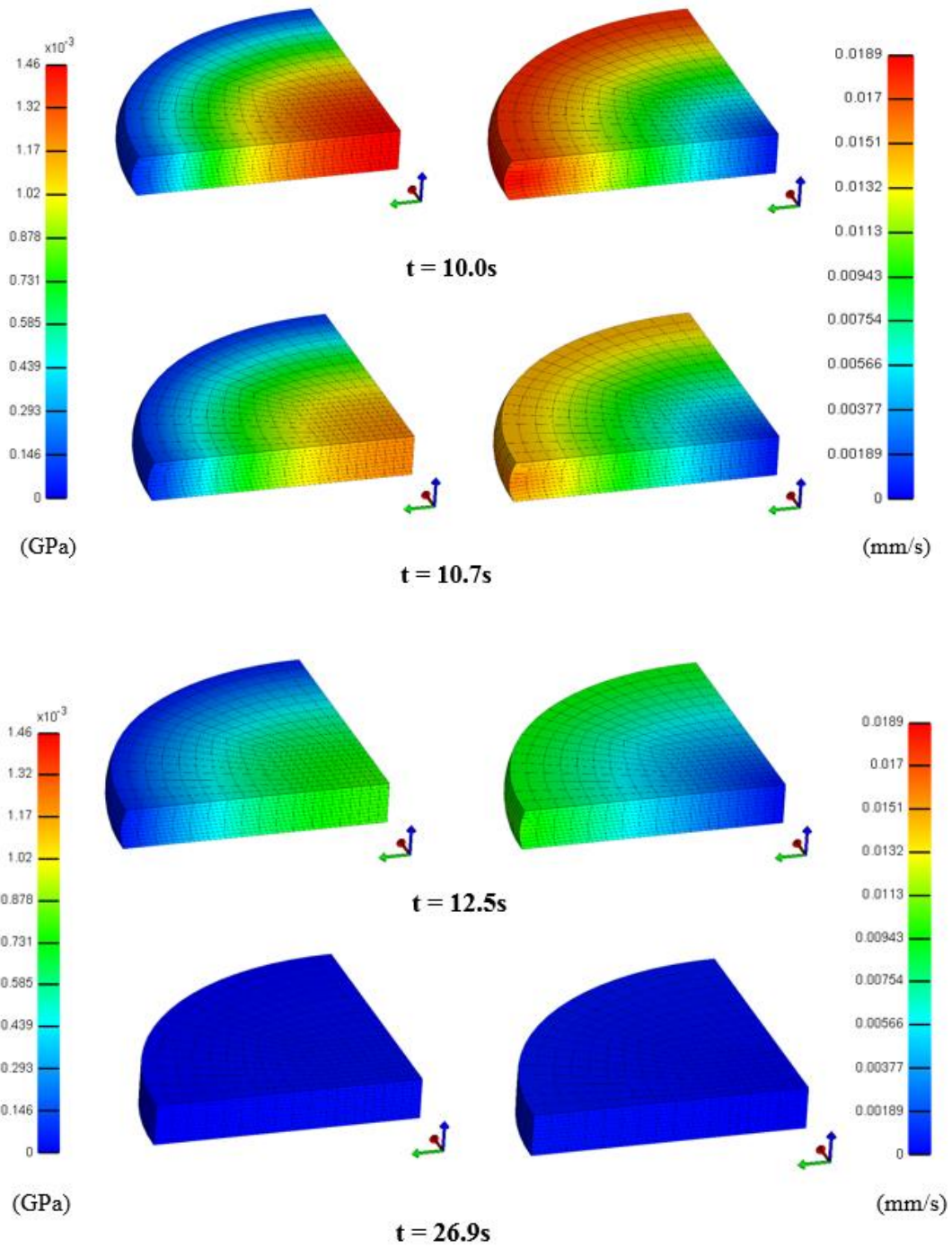


Figure 5.17.1: Fluid pressure (first column) and fluid flux (second column) gradients in a 3.2% collagen gel undergoing unconfined ramp-hold compression. Ramp displacement rate is 1%/sec and holds for 10sec.

# APPENDIX R

## *Results*

### Material Parameters

Material parameters and determination coefficient ( $R^2$ ) for 9 samples of 2.9% collagen. Optimisation was performed by fitting the hold phase of the experimental curve. Sample I was excluded.

<b>Sample Name</b>	<b>Young's Modulus <math>E</math> (Pa)</b>	<b>Zero-Strain Hydraulic Permeability <math>k</math> (mm<sup>4</sup>/Ns)</b>	<b>Non-Linear Permeability Coefficient <math>M</math> (mm<sup>4</sup>/Ns)</b>	<b>Determination Coefficient <math>R^2</math></b>
A	902	32.3	9.67	0.976
B	521	28.5	6.09	0.950
C	985	40.4	11.0	0.917
D	1113	52.6	18.1	0.923
E	1109	27.0	3.79	0.869
F	497	64.0	8.29	0.893
G	962	79.5	22.6	0.958
H	1068	94.7	21.8	0.940
J	137	43.2	5.47	0.728
<b>Average</b>	<b>810</b>	<b>51.4</b>	<b>11.9</b>	<b>-</b>
<b>STDEV</b>	<b>343</b>	<b>23.7</b>	<b>7.16</b>	<b>-</b>

Table 5.18.1: Material parameters and determination coefficient ( $R^2$ ) for 2.9% collagen samples.

Material's parameters and determination coefficient ( $R^2$ ) for 10 samples of 3.2% collagen. Optimization was performed by fitting the hold phase of the experimental curve.

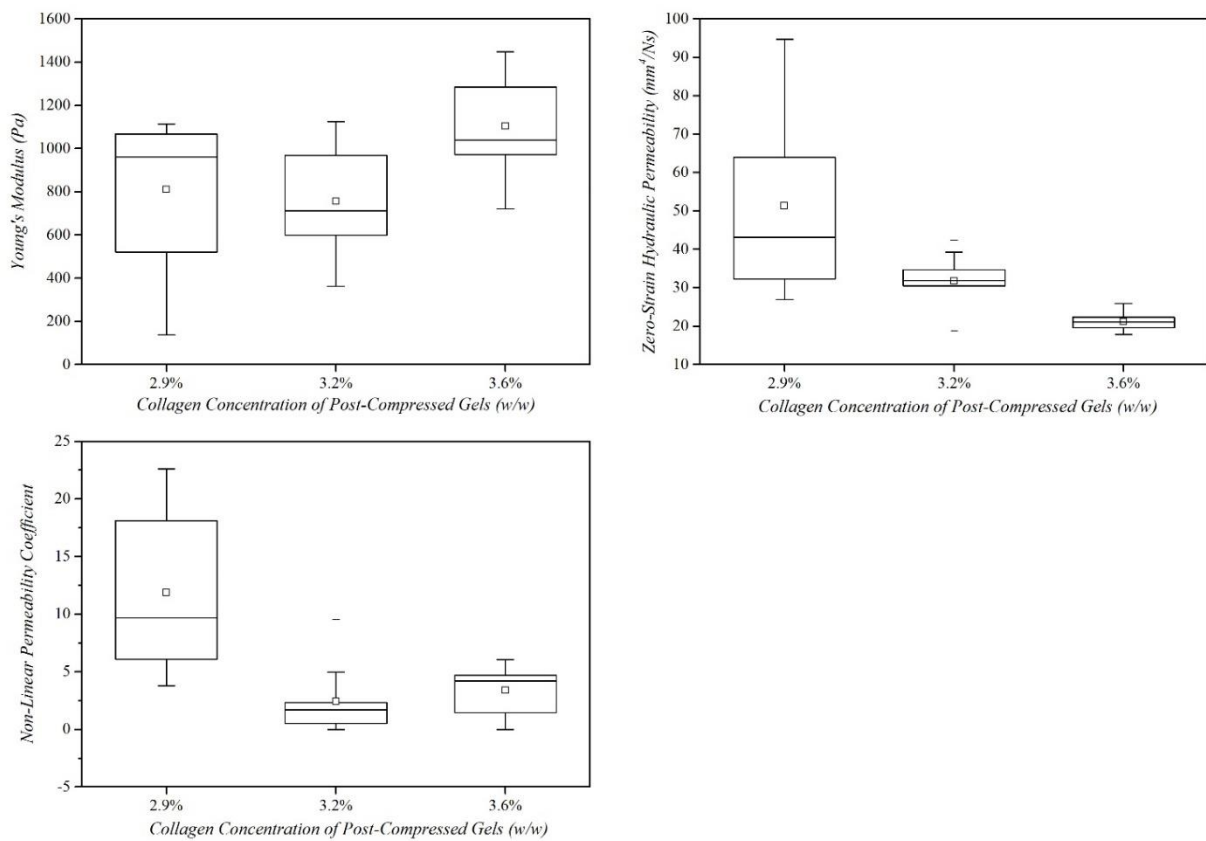
Sample Name	Young's Modulus $E$ (Pa)	Zero-Strain Hydraulic Permeability $k$ ( $\text{mm}^4/\text{Ns}$ )	Non-Linear Permeability Coefficient $M$ ( $\text{mm}^4/\text{Ns}$ )	Determination Coefficient $R^2$
A	761	33.3	2.31	0.948
B	732	32.1	1.54	0.970
C	1069	18.7	0.50	0.963
D	1124	34.7	9.55	0.981
E	694	39.3	1.86	0.938
F	599	30.5	0.001	0.937
G	969	24.0	1.10	0.966
H	674	31.6	4.97	0.949
I	568	31.0	2.19	0.967
J	363	42.4	0.001	0.947
<b>Average</b>	<b>755</b>	<b>31.8</b>	<b>2.40</b>	-
<b>STDEV</b>	<b>237</b>	<b>6.78</b>	<b>2.90</b>	-

Table 5.18.2: Material's parameters and determination coefficient ( $R^2$ ) for 3.2% collagen samples.

Material's parameters and determination coefficient ( $R^2$ ) for 10 samples of 3.6% collagen. Optimization was performed by fitting the hold phase of the experimental curve.

Sample Name	Young's Modulus $E$ (Pa)	Zero-Strain Hydraulic Permeability $k$ ( $\text{mm}^4/\text{Ns}$ )	Non-Linear Permeability Coefficient $M$ ( $\text{mm}^4/\text{Ns}$ )	Determination Coefficient $R^2$
A	1333	21.4	6.05	0.954
B	1449	17.9	4.70	0.952
C	1284	22.0	4.51	0.966
D	1045	22.4	1.87	0.970
E	722	25.9	0.001	0.946
F	996	20.8	4.42	0.929
G	1236	20.6	5.61	0.947
H	972	19.6	1.29	0.961
I	1035	18.5	1.45	0.949
J	961	22.8	4.02	0.939
<b>Average</b>	<b>1103</b>	<b>21.2</b>	<b>3.39</b>	-
<b>STDEV</b>	<b>217</b>	<b>2.31</b>	<b>2.07</b>	-

Table 5.18.3: Material's parameters and determination coefficient ( $R^2$ ) for 3.6% collagen samples.



Box Chart 5.18.1: Young's modulus, Zero-strain hydraulic permeability and Non-linear permeability coefficient for 2.9, 3.2 and 3.6% collagen samples. □ implies the mean value.

# APPENDIX S

## Results

### Dynamic Mechanical Analysis (DMA)

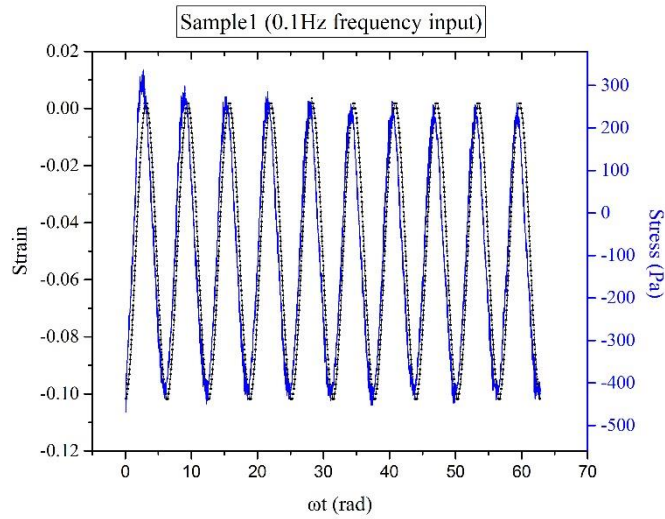


Figure 5.19.1: Dynamic loading of a 3.2% collagen gel at 0.1Hz frequency. Black curve is the strain input and blue curve is the stress output.

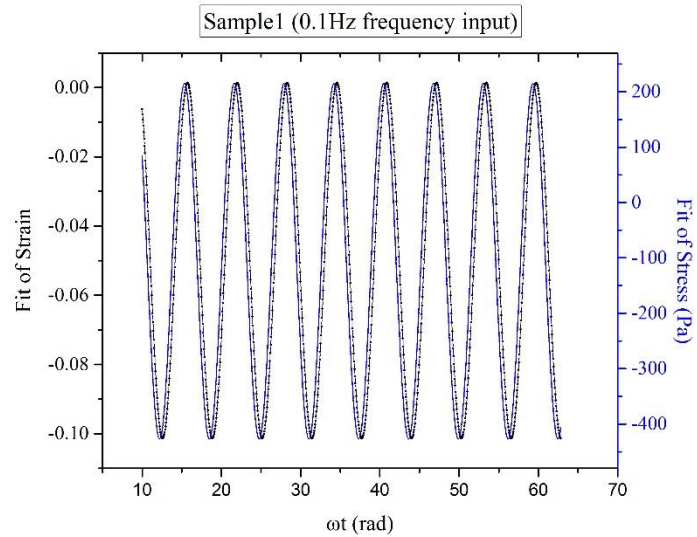


Figure 5.19.2: Fit of experimental data obtained from dynamic loading of a 3.2% collagen gel at 0.1Hz frequency. Black curve is the fit of strain input and blue curve is the fit of stress output.

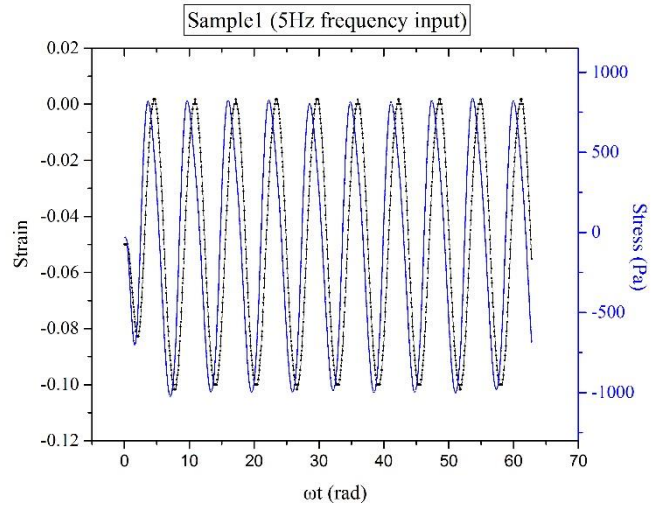


Figure 5.19.3: Dynamic loading of a 3.2% collagen gel at 5Hz frequency. Black curve is the strain input and blue curve is the stress output.

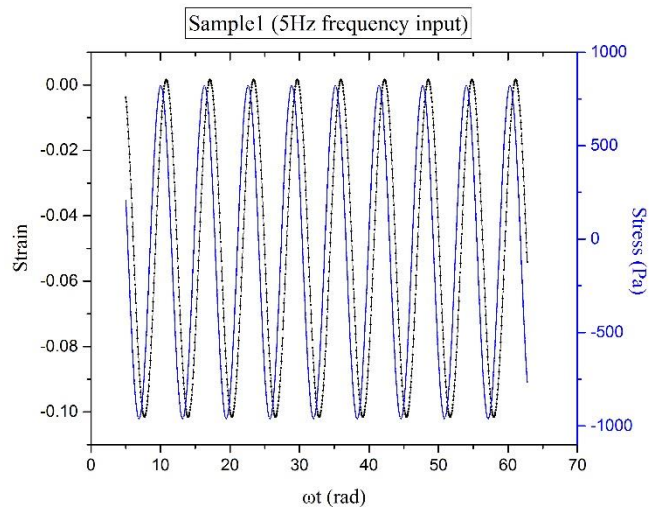


Figure 5.19.4: Fit of experimental data obtained from dynamic loading of a 3.2% collagen gel at 5Hz frequency. Black curve is the fit of strain input and blue curve is the fit of stress output.

Frequency (Hz)	Phase lag $\delta$ (deg)	Tan $\delta$	Complex Modulus (Pa)	Storage Modulus (Pa)	Loss Modulus (Pa)
0.1	0.39	0.41	7,095	6,559	2,700
0.5	0.50	0.55	10,024	8,802	4,796
1	0.58	0.65	11,351	9,503	6,207
2	0.67	0.80	14,269	11,171	8,876
5	0.78	0.99	18,593	13,199	13,083

Table 5.19.1: Phase lag ( $\delta$ ), complex, storage and loss moduli of a 3.2% collagen gel at different frequencies.



# 1 REFERENCES

---

- Argoudi, M., and A. Shirazi-Adl. "Poroelastic Creep Response Analysis of a Lumbar Motion Segment in Compression." *Journal of Biomechanics* 29: 1331–39, 1996.
- Ateshian, G. A., W. H. Warden, R. P. Kim, R. P. Grelsamer, and V. C. Mow. "Finite Deformation Biphasic Material Properties of Bovine Articular Cartilage from Confined Compression Experiments." *Journal of Biomechanics* 30: 1157–1164, 1997.
- Barocas, V. H., and R. T. Tranquillo. "An Anisotropic Biphasic Theory of Tissue-Equivalent IVIeclianics: The Interplay Among Cell Traction, Fibrillar Network Deformation, Fibril Alignment, and Cell Contact Guidance." *Journal of Biomechanical Engineering*, 1997.
- Bernich, E., R. Rubenstein, and J. S. Bellin. "Membrane Transport Properties of Bovine Articular Cartilage." *Biochim Biophys Acta* 448: 551-561, 1976.
- Blais, M., R. Parenteau-Bareil, S. Cadau, and F. Berthod. "Concise Review: Tissue-Engineered Skin and Nerve Regeneration in Burn Treatment." *Stem Cells Transl Med* 2(7): 545-51, 2013.
- Brown, R. A., M. Wiseman, C. B. Chuo, U. Cheema, and S. N. Nazhat. "Ultrarapid Engineering of Biomimetic Materials and Tissues: Fabrication of Nano- and Microstructures by Plastic Compression." *Advanced Functional Materials* 15: 1762-1770, 2005.
- Busby, G. A., M. H. Grant, S. P. MacKay, and P. E. Riches. "Confined Compression of Collagen Hydrogels." *Journal of Biomechanics* 46: 837–840, 2013.
- Chandran, P. L., and V. H. Barocas. "Microstructural Mechanics of Collagen Gels in Confined Compression: Poroelasticity, Viscoelasticity and Collapse." *J Biomech Eng* 126(2): 152-66, 2004.
- Cheema, U., and R. A. Brown. "Rapid Fabrication of Living Tissue Models by Collagen Plastic Compression: Understanding Three-Dimensional Cell Matrix Repair In Vitro." *Adv Wound Care* 2(4): 176–184, 2013.
- Chiang, H., and C. C. Jiang. "Repair of Articular Cartilage Defects: Review and Perspectives." *J Formos Med Assoc* 108(2): 87-101, 2009.
- Chicatun, F, et al. "Osteoid-Mimicking Dense Collagen/Chitosan Hybrid Gels." *Biomacromolecules* 12(8): 2946-56, 2011.
- Cui, Fu-Zhai, Yan Li, and Jun Ge. "Self-Assembly of Mineralized Collagen Composites." *Materials Science and Engineering R* 57: 1-27, 2007.
- De Moraes, M. A., E. Paternotte, D. Mantovani, and M. M. Beppu. "Mechanical and Biological Performances of New Scaffolds Made of Collagen Hydrogels and Fibroin Microfibers for Vascular Tissue Engineering." *Macromol Biosci* 12: 1253–1264, 2012.

- Farrell, M D. *Experimental and Finite Element Analysis of Mechano-Electrochemical Effects in Intervertebral Disc Biomechanics* . Glasgow, 2013.
- Gentleman, E., A. N. Lay, D. A. Dickerson, E. A. Nauman, G. A. Livesay, and K. C. Dee. “Mechanical Characterisation of Collagen Fibers and Scaffolds for Tissue Engineering.” *Biomaterials* 24: 3805–3813, 2003.
- Ghezzi, C. E., B. Marelli, N. Muja, and S. N. Nazhat. “Immediate Production of a Tubular Dense Collagen Construct with Bioinspired Mechanical Properties.” *Acta Biomaterialia* 8: 1813–1825, 2012.
- Happel, J. “Viscous Flow Relative to Arrays of Cylinders.” *AIChE Journal* 5: 174–177, 1959.
- Holmes, M. H., and V. C. Mow. “The nonlinear characteristics of soft gels and hydrated connective tissues in ultrafiltration.” *Journal of Biomechanics* 23: 1145–56, 1990.
- Jeong, S. I., et al. “Tissue-Engineered Vascular Grafts Composed of Marine Collagen and PLGA Fibers using Pulsatile Perfusion Bioreactors.” *Biomaterials* 28: 1115–1122, 2007.
- Kew, S. J., et al. “Regeneration and Repair of Tendon and Ligament Tissue using Collagen Fibre Biomaterials.” *Acta Biomaterialia* 7: 3237–3247, 2011.
- Knapp, D. M., V. H. Barocas, and A. G. Moona. “Rheology of Reconstituted Type I Collagen Gel in Confined Compression.” *J Rheol* 41: 971 , 1997.
- Lai, E. S., C. M. Anderson, and G. G. Fuller. “Designing a Tubular Matrix of Oriented Collagen Fibrils for Tissue Engineering.” *Acta Biomaterialia* 7: 2448–2456, 2011.
- Lai, W. M., and V. C. Mow. “Drag-Induced Compression of Articular Cartilage during a Permeation Experiment.” *Biorheology* 17: 111–123, 1980.
- Marelli, B., C. E. Ghezzi, J. E. Barralet, and S. N. Nazhat. “Collagen Gel Fibrillar Density Dictates the Extent of Mineralization in vitro.” *Soft Matter* 7: 9898, 2011.
- Maroudas, A. “Physicochemical Properties of Articular Cartilage.” *In Adult Articular Cartilage pp.215-29. Pitman Medical, London, 1979.*
- Matsuda, K., S. Suzuki, N. Isshiki, K. Yoshioka , T. Okada, and Y. Ikada. “Influence of Glycosaminoglycans on the Sponge Component of a Bilayer Artificial Skin.” *Biomaterials* 11: 351–355, 1990.
- Mow, V. C., S. C. Kuei, W. M. Lai, and C. G. Armstrong. “Biphasic Creep and Stress Relaxation of Articular Cartilage in Compression: Theory and Experiments.” *Journal of Biomech Eng* 102: 73–84, 1980.
- Neel, E. A., U. Cheema, J. C. Knowles, R. A. Brown, and S. N. Nazhat. “Use of Multiple Unconfined Compression for Control of Collagen Gel Scaffold Density and Mechanical Properties.” *Soft Matter* 2: 986–992, 2006.

- Orban, J. M., L. B. Wilson, J. A. Kofroth, M. S. El-Kurdi, T. M. Maul, and D. A. Vorp. "Crosslinking of Collagen Gels by Transglutaminase." *J Biomed Mater Res A* 68(4): 756-62, 2004.
- Perie, D., D. Korda, and J. C. Iatridis. "Confined Compression Experiments on Bovine Nucleus Pulposus and Annulus Fibrosus: Sensitivity of the Experiment in the Determination of Compressive Modulus and Hydraulic Permeability." *J Biomech* 38: 2164-71, 2005.
- Ratner, B. D., A. S. Hoffman, F. J. Schoen, and J. E. Lemons. *An Introduction to Materials in Medicine*. Biomaterials Science, 1996.
- Rich, H., M. Odlyha, U. Cheema, V. Mudera, and L. Bozec. "Effects of Photochemical Riboflavin-Mediated Crosslinks on the Physical Properties of Collagen Constructs and Fibrils." *J Mater Sci: Mater Med* 25: 11–21, 2014.
- Riches, P. E., N. Dhillon, J. Lotz, A. W. Woods, and D. S. McNally. "The internal mechanics of the intervertebral disc under cyclic loading." *Journal of Biomechanics* 35: 1263–71, 2002.
- Saddiq, Z. A., J. C. Barbenel, and M. H. Grant. "The Mechanical Strength of Collagen Gels Containing Glycosaminoglycans and Populated with Fibroblasts." *J Biomed Mater Res A*. 89(3): 697-706, 2009.
- Serpooshan, V., et al. "Reduced Hydraulic Permeability of Three-Dimensional Collagen Scaffolds Attenuates Gel Contraction and Promotes the Growth and Differentiation of Mesenchymal Stem Cells." *Acta Biomaterialia* 6: 3978–3987, 2010.
- Serpooshan, V., T. M. Quinn, N. Muja, and S. N. Nazhat. "Characterization and Modelling of a Dense Lamella Formed during Self-Compression of Fibrillar Collagen Gels: Implications for Biomimetic Scaffolds." *Soft Matter* 7: 2918–26, 2011.
- Serpooshan, V., T. M. Quinn, N. Muja, and S. N. Nazhat. "Hydraulic Permeability of Multilayered Collagen Gel Scaffolds under Plastic Compression-Induced Unidirectional Fluid Flow." *Acta Biomaterialia* 9: 4673–4680, 2013.
- Siemionow, M., M. Bozkurt, and F. Zor. "Regeneration and Repair of Peripheral Nerves with Different Biomaterials: Review." *Microsurgery* 30(7): 574-88, 2010.
- Swartz, M. A., and M. E. Fleury. "Interstitial Flow and its Effects in Soft Tissues." *Ann Rev Biomed Eng* 9: 229–56, 2007.
- Tabata, Yasuhiko . "Biomaterial technology for tissue engineering applications." *J R Soc Interface* 6: S311–S324, 2009.
- Thottappillil, N., and P. D. Nair. "Scaffolds in Vascular Regeneration: Current Status." *Vascular Health and Risk Management* 11: 79–91, 2015.
- Urban, J. P. G., and S. H. Holm. "Intervertebral Disc Nutrition as Related to Spinal Movements and Fusion." *In Tissue Nutrition and Viability* pp. 101-119. Springer, New York, 1986.

Willoughby , C. E., M. Batterbury , and S. B. Kaye. "Collagen Corneal Shields." *Surv Ophthalmol.* 47(2): 174-82, 2002.

Zeeman, R., et al. "Crosslinking and Modification of Dermal Sheep Collagen." *J Biomed Mater Res* 46(3): 424-33, 1999.

Zerris, V. A., K. S. James, J. B. Roberts, E. Bell, and C. B. Heilman. "Repair of the Dura Mater With Processed Collagen Devices." *J Biomed Mater Res B Appl Biomater.* 83(2): 580-8, 2007.

## Web Source

[1] <http://users.ics.forth.gr/~lourakis/levmar/>